Preprints.org

Article

Not peer-reviewed version

# Acidic Oxidative Depolymerization Towards Functionalized Low Molecular Weight Lignin and High Value-Added Aliphatic Monomers: Operating Conditions, Scale-Up, and Crosslinking

Marta C. Lourenço , Talita Nascimento , Pedro Miguel Sanches Filho , Ana C. Marques * , Marta Ramos-Andrés *

Posted Date: 31 March 2025

doi: 10.20944/preprints202503.2415.v1

Keywords: Lignoboost; hydrogen peroxide; dicarboxylic acids; functionalization; Kraft lignin

Preprints.org is a free multidisciplinary platform providing preprint service that is dedicated to making early versions of research outputs permanently available and citable. Preprints posted at Preprints.org appear in Web of Science, Crossref, Google Scholar, Scilit, Europe PMC.

Copyright: This open access article is published under a Creative Commons CC BY 4.0 license, which permit the free download, distribution, and reuse, provided that the author and preprint are cited in any reuse.

Preprints.org (www.preprints.org) | NOT PEER-REVIEWED | Posted: 31 March 2025 doi:10.20944/preprints202503.2415.v1

Disclaimer/Publisher's Note: The statements, opinions, and data contained in all publications are solely those of the individual author(s) and contributor(s) and not of MDPI and/or the editor(s). MDPI and/or the editor(s) disclaim responsibility for any injury to people or property resulting from any ideas, methods, instructions, or products referred to in the content.

*Article*

# Acidic Oxidative Depolymerization Towards Functionalized Low Molecular Weight Lignin and High Value-Added Aliphatic Monomers: Operating Conditions, Scale-Up, And Crosslinking

**Marta C. Lourenço [1], Talita Nascimento [1], Pedro José Sanches Filho [2], Ana C. Marques [3,*] and Marta Ramos-Andrés [1,*]**

[1] Centro de Recursos Naturais e Ambiente (CERENA), Instituto Superior Técnico, Universidade de Lisboa, Av. Rovisco Pais, 1049-001 Lisbon, Portugal

[2] Centro de Química Estrutural (CEQ), Instituto Superior Técnico, Universidade de Lisboa, Av. Rovisco Pais, 1049-001 Lisbon, Portugal

[3] CERENA, Department of Chemical Engineering, Instituto Superior Técnico, Universidade de Lisboa, Avenida Rovisco Pais, 1049-001 Lisboa, Portugal

* Correspondence: ana.marques@tecnico.ulisboa,pt (Ana C. Marques); marta.ramos@tecnico.ulisboa.pt (Marta Ramos-Andrés)

**Abstract:** Lignin, a complex aromatic biopolymer abundant as waste in biorefineries and the pulp and paper industry, holds significant potential for valorization. This study presents the oxidative depolymerization of Lignoboost lignin (LB) using $H_2O_2$ under mild, solvent- and catalyst-free, inherently acidic conditions at temperatures from 50-70°C. The depolymerized LB was rich in aromatic dimers-trimers (68.6 wt.%) with high functionalization (2.75 mmol/g OHphen, 3.58 mmol/g OHcarb, 19.5 wt.% of H in -CH=CH-), and aliphatic dicarboxylic acids (53.4 wt.% of the monomers). Acidic conditions provided higher depolymerization and functionalization than alkaline conditions, alongside simplified product recovery. The process was also successfully applied to Kraft lignin (KL) from black liquor, demonstrating its versatility and robustness. The optimized conditions were scaled up (×25), improving efficiency and yielding a Mw and Đ of 464 g/mol and 1.3, respectively. As proof of concept, the scaled-up product underwent radical crosslinking, resulting in a new biopolymer with higher thermal stability than LB (54.2 wt.% residual mass at 600°C *versus* 36.1 wt.%). This green, scalable depolymerization process enhances lignin valorization, producing two high-value compounds—low molecular weight functionalized aromatics and dicarboxylic acids—that can be used independently or together, owing to their inherent capacity to form crosslinked networks.

**Keywords:** Lignoboost; hydrogen peroxide; dicarboxylic acids; functionalization; Kraft lignin

## 1. Introduction

Lignin, the most abundant aromatic biopolymer in lignocellulosic biomass, is a significant component of the waste stream in biorefineries, particularly in the paper and bioethanol industries. Traditionally considered a waste product [1,2], lignin holds great potential for valorization due to its high carbon content and aromatic structure, which makes it an attractive candidate for various applications, including biofuels, chemicals, and materials .

Kraft lignin (KL), derived from the Kraft pulping process, is one of the most studied types of lignin. However, it is characterized by a high molecular weight and inherent heterogeneity, making it poorly reactive and difficult to dissolve [3]. Moreover, KL typically contains higher levels of impurities, such as carbohydrates and inorganic compounds, which affect its reactivity [4]. As a result, KL often requires further processing to enhance its usability for a range of applications. In contrast, the Lignoboost process, a novel technique for lignin recovery, yields a lignin of higher purity

© 2025 by the author(s). Distributed under a Creative Commons CC BY license.

Preprints.org (www.preprints.org) | NOT PEER-REVIEWED | Posted: 31 March 2025 doi:10.20944/preprints202503.2415.v1



and quality. The process involves the precipitation of lignin from black liquor using $CO_2$, followed by intensive washing at pH 2 to remove residual impurities [5]. This approach results in a lignin with a more protonated character, which improves its reactivity and makes it more suitable for functionalization [6].

The main challenge with lignin lies in its complex, heterogeneous structure, which leads to low reactivity and poor solubility. Reducing its molecular weight offers several benefits, including reduced steric hindrance, decreased heterogeneity, increased reactivity, and improved solubility. The phenolic hydroxyl groups (OHphen) present in lignin are the most abundant and reactive functional groups [7]. Preserving these groups during depolymerization is crucial for maintaining lignin's reactivity. Oxidative depolymerization is an effective method to achieve this goal, as it can partially preserve OHphen groups while generating new functional groups, particularly carboxylic hydroxyl groups (OHcarb), which are highly reactive and have potential applications in processes like crosslinking [8]. In addition, oxidative depolymerization leads to the formation of alkene groups (aliphatic double bonds), which, when adjacent to C-C bonds, form vinyl groups that are highly reactive in radical polymerization reactions [9]. In addition to low-molecular-weight functionalized aromatics, one of the most common derivatives obtained from oxidative depolymerization are dicarboxylic acids, which can be generated through the cleavage of the aromatic ring [10]. These molecules have wide-ranging industrial applications, particularly in the synthesis of polyesters or biopolyesters.

Various methods for lignin oxidative depolymerization have been extensively studied, with hydrogen peroxide ($H_2O_2$) emerging as one of the most promising oxidizing agents due to its accessibility, low cost, and environmentally friendly byproducts (water and oxygen). Previous studies have shown that $H_2O_2$ can depolymerize lignin under both acidic and alkaline conditions under different mechanisms [11]. One of the key differences lies in the solubility of lignin; while it is insoluble in acidic environments, it becomes soluble in alkaline conditions.

Previous studies have explored the oxidative depolymerization of lignin with $H_2O_2$ for functionalization while preserving the oligomeric structure. Ahmad et at. (2020) successfully depolymerized KL under inherent acidic conditions and ambient temperature, achieving functionalization and molecular weight reduction, leading to functionalized oligomers [12]. Junghans et al. (2020) reported alkaline oxidative depolymerization with diluted $H_2O_2$ at moderate temperatures (30-90°C), achieving an 82% molecular weight reduction through side chains cleavage while preserving β-O-4 linkages. The oligomers were functionalized with increased COOH content (2.66 mmol/g) [13]. Ruwoldt et al. (2025) performed alkaline oxidation with $H_2O_2$ to convert OHphen groups into OHcarb, but this process did not lead to depolymerization and instead lignin's molecular weight increase, although enhancing its solubility for emulsifier applications [14].

The advantages of acidic over alkaline depolymerization prompted Kim et al. (2020) to study the depolymerization of lignin by combining acetic acid with $H_2O_2$ [15]. This combination allowed for aromatic ring cleavage and COOH incorporation, producing polycarboxylates with applications as plasticizers. Li et al. (2020) employed $H_2O_2$ with formic acid and a mineral acid catalyst to cleavage C-C and β-O-4 linkages at ambient temperature, generating aromatic monomers (phenoxy-methyl benzoate, benzoic acid, and phenol) as the main products (90%) [16]. More recently, Andriani and Lawoko (2024) combined acetic acid and $H_2O_2$, finding that ring cleavage led to the formation of muconic acid- and ester-end groups and at the same time keeping the macromolecular structure of the lignin intact, but in an oxidized form, resulting in the recovery of multifunctionalized oligomers with COOH groups [3]. These oligomers were less dispersed than the original lignin and exhibited more hydrophilic characteristics.

Regarding the generation of low-molecular-weight aliphatic derivatives, catalysts have often been employed to enhance production. Vega-Aguilar et al. (2021) studied the production of C4 dicarboxylic acids by oxidizing various lignins with $H_2O_2$ and titanium silicalite-1 as a catalyst [17]. This enabled the production of succinic acid as the major compound. Sun et al. (2023) studied the electrochemical conversion of lignin into short-chain carboxylic acids using $H_2O_2$ with titanium

Preprints.org (www.preprints.org) | NOT PEER-REVIEWED | Posted: 31 March 2025 doi:10.20944/preprints202503.2415.v1



silicate-1 as a catalyst, generating $H_2O_2$ in situ [18]. Bi et al. (2018) also studied lignin degradation into dicarboxylic acids using $CuFeS_2$ nanoparticles as a catalyst in combination with $H_2O_2$, with oxalic acid being the major product (30 % selectivity) [19].

To the best of our knowledge, no other research group has fully described the acidic oxidative depolymerization of lignin under the specific conditions of high $H_2O_2$ concentration, high lignin concentration, and without the addition of external acids, co-solvents, or catalysts. This process achieves high efficiency in obtaining depolymerized/functionalized lignin, along with dicarboxylic acids. The acidic environment is created through the inherent protonated character of LB, which is suspended at a high concentration in water. This simplifies product recovery via simple drying and enhances scalability. This recovery method ensures that all derivatives formed during depolymerization are preserved without loss, a common issue in processes that involve precipitation. The present study investigates the effects of temperature and time on LB depolymerization, as well as the impact of operating under inherent acidic versus alkaline conditions, and the influence of stirring in acidic conditions. The optimized process was applied to both LB and KL, identifying the necessary adjustment for adapting the process to less pure lignins. Finally, the process was successfully scaled up by a factor of 25, incorporating improvements that resulted in a higher degree of depolymerization. As proof of concept, the depolymerized products were crosslinked by free-radical reactions, leading to a derivative with significantly enhanced thermal stability, making it a promising candidate for future studies and a wide range of applications.

## 2. Results and Discussion

### *2.1. Acidic Oxidative Depolymerization/Functionalization Under Different Temperatures*

#### 2.1.1. Evolution of the Molecular Weight Distribution

The molecular weight distribution of the acidic oxidative depolymerization at the three operational temperatures (Figure 1.A) showed the emergence of two distinct peaks corresponding to lower molecular weights. The first peak, located around 150 g/mol, was associated with the monomers presence and initially increased in the samples, gradually decreasing thereafter. Typical lignin monomers with molecular weights near 150 g/mol include vanillin (152 g/mol), vanillic acid (168 g/mol), coumaric acid (164.05 g/mol), malic acid (134.10 g/mol) and succinic acid (118.10 g/mol), among others. The second peak, around 300 g/mol, likely corresponds to dimers or trimers, depending on the level of functionalization of the molecules. This peak consistently increased over time. When comparing the temperatures, it can be observed that the distribution obtained at 50°C after 7 h was very similar to that achieved at 60°C after just 3 h. In contrast, at 70°C, only 2 h were required to reach a distribution that appeared stable. This distribution displayed the highest degree of depolymerization, with a greater increase in the monomer and dimers-trimers peaks and a more significant reduction in the oligomeric region.

Preprints.org (www.preprints.org) | NOT PEER-REVIEWED | Posted: 31 March 2025 doi:10.20944/preprints202503.2415.v1



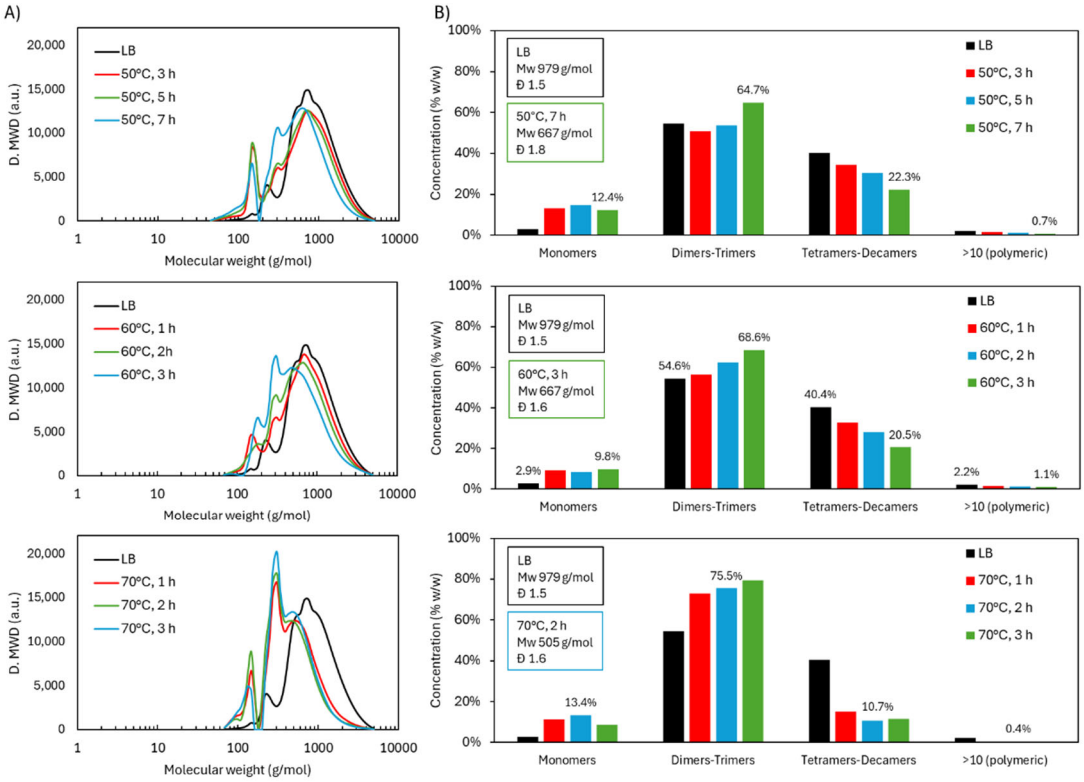


**Figure 1.** Molecular weight distribution of LB during acidic oxidative depolymerization under different temperatures: A) GPC chromatograms and B) distribution in molecular groups.

The proportion of different molecular groups (Figure 1.B) was estimated following the method described in section 4.4. The results show that the monomers increased slightly, reaching a maximum of 15.8 wt.% after 50°C-5h. In the later samples, a slight decrease was observed, which could be attributed to possible repolymerization processes. On the other hand, the dimers-trimers fraction increased over time, reaching 64.7 wt.% (50°C-7 h), 68.6 wt.% (60°C, 3 h), and 75.5 wt.% (70°C, 2 h). The group of tetramers-decamers showed a marked decrease, which was more pronounced at higher temperatures, decreasing from 40.4 wt.% in the original lignin to a minimum of 22.3 wt.% (50°C, 7 h), 20.5 wt.% (60°C, 3 h), and 10.7 wt.% (70°C, 2 h). The polymeric fraction was consistently minor, with percentages below 1.1 wt.%.

These results demonstrate an effective depolymerization process, where the monomers are not the majority compounds. However, dimers-trimers molecules reach a very high proportion, thereby increasing the homogeneity of the lignin-based material and reducing its steric hindrance. Furthermore, this process successfully led to the presence of more and new functional groups, as will be discussed in the next section.

### 2.1.2. Structural Characterization (ATR-FTIR, $^{1}$H NMR, $^{31}$P NMR, EA, TGA, GC-FID/(TOF-MS))

To better understand the evolution of functional groups during acidic oxidative depolymerization of lignin, structural characterization was performed using multiple complementary techniques.

ATR-FTIR analysis (Figure 2) showed that OH bands (3600–3000 $cm^{-1}$) [20] remained present in all depolymerized samples, although shifts in OH types were later confirmed through NMR. Peaks corresponding to aliphatic C–H stretching in $CH_2$ and $CH_3$ groups (2938, 2842 $cm^{-1}$) [21] were consistently observed, with slightly broader signals at 70 °C, possibly reflecting increased functional group diversity.

Preprints.org (www.preprints.org) | NOT PEER-REVIEWED | Posted: 31 March 2025 doi:10.20944/preprints202503.2415.v1



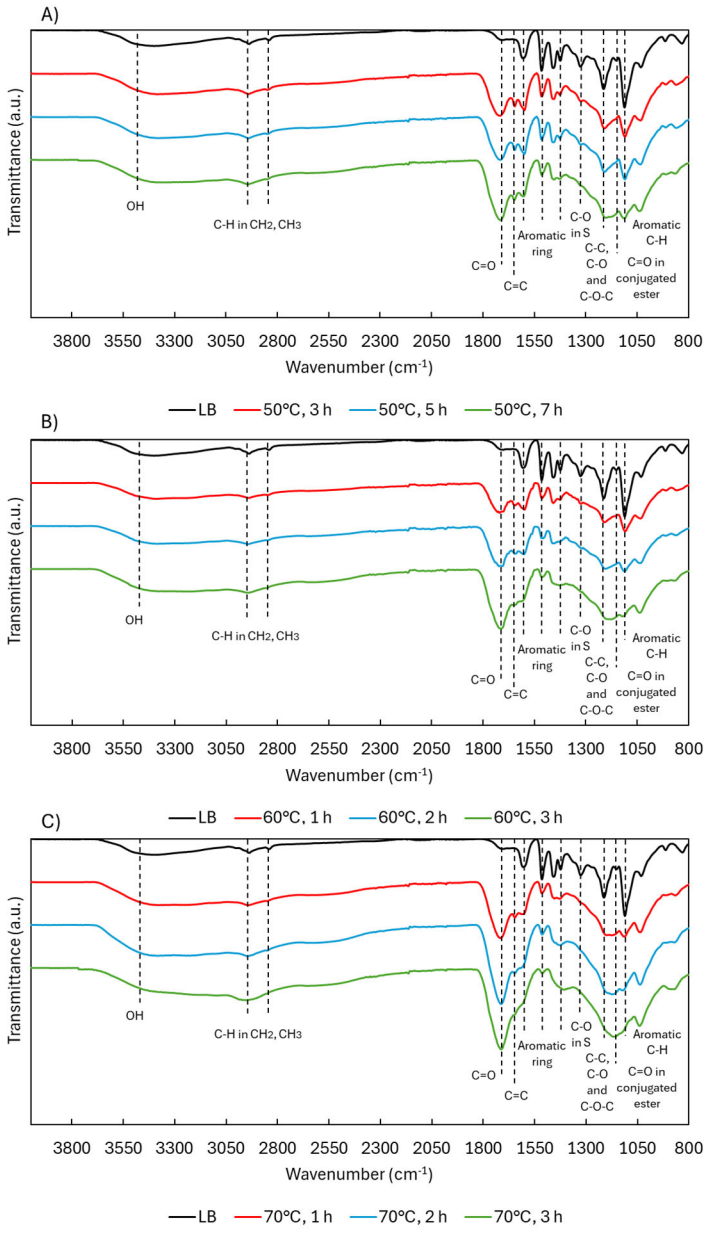


**Figure 2.** ATR-FTIR spectra of LB during acidic oxidative depolymerization under different temperatures.

The most prominent change occurred at 1714 $cm^{-1}$, where the carbonyl (C=O) band [12] increased in intensity with both temperature and time. This is likely due to the formation of carboxylic acids, ketones, aldehydes, and esters, generated through oxidative cleavage of ether linkages and side chains. A new band at 1642 $cm^{-1}$, attributed to aliphatic C=C bonds [22], appeared under all conditions but was most intense at lower temperatures. These alkenes likely form through ring cleavage or the creation of quinonoid structures, as illustrated in Figure 3, and are relevant markers of lignin reactivity.

Preprints.org (www.preprints.org) | NOT PEER-REVIEWED | Posted: 31 March 2025 doi:10.20944/preprints202503.2415.v1



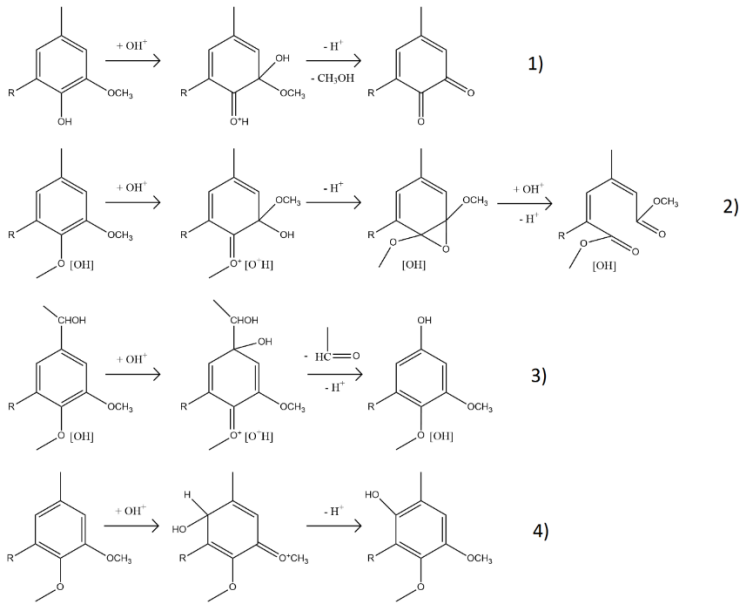


**Figure 3.** Mechanisms of acidic oxidative depolymerization of lignin with hydroxonium ions: 1) demethoxylation, 2) ring cleavage, 3) displacement of side chains, and 4) ring hydroxylation. Adapted from Gierer (1986).

The three primary aromatic bands at 1604, 1515, and 1424 $cm^{-1}$ [12] remained largely unchanged for the first two peaks, indicating the aromatic backbone was mostly preserved despite depolymerization. The 1424 $cm^{-1}$ band, however—associated with in-plane ring deformation—decreased notably and disappeared at higher temperatures, possibly due to substitution pattern changes or side-chain removal.

The syringyl (S) C–O band at 1323 $cm^{-1}$ [12] also decreased, suggesting demethoxylation via $OCH_3$ loss. The region around 1214 $cm^{-1}$ (C–C, C–O, and C–O–C) [21,23] remained present but began overlapping with the 1145 $cm^{-1}$ band, which increased with temperature and is assigned to esters conjugated with aromatics or unsaturated systems [24]. This suggests ester formation via ring cleavage or acid-catalyzed esterification between COOH and OH groups. Supporting this, the 1132 $cm^{-1}$ peak (aromatic C–H in-plane deformation) [25] gradually decreased, though never fully disappeared, pointing to progressive side-chain removal.

$^{31}P$ NMR analyses (Figure 4.A) provided a clearer view of how specific OH groups evolved with depolymerization severity, expressed as $logR_0$. For $logR_0 < 4.5$, $^{31}P$ NMR showed a decline in both OHphen and OHaliph groups, alongside a substantial increase in OHcarb, suggesting oxidation of OH groups into acids or quinones. As severity increased beyond $logR_0 = 4.5$, OHphen slightly recovered, while OHcarb plateaued, indicating that further oxidation was limited under these conditions. At 60 °C for 3 h ($logR_0 = 4.5$), the OH content shifted from 0.35 to 3.58 mmol/g (OHcarb), 4.31 to 2.74 mmol/g (OHphen), and 1.53 to 0.78 mmol/g (OHaliph), with OHtotal increasing from 6.20 to 7.10 mmol/g. These results demonstrate an effective functionalization process (COOH, C=C) while largely preserving the OHphen groups.

Preprints.org (www.preprints.org) | NOT PEER-REVIEWED | Posted: 31 March 2025 doi:10.20944/preprints202503.2415.v1



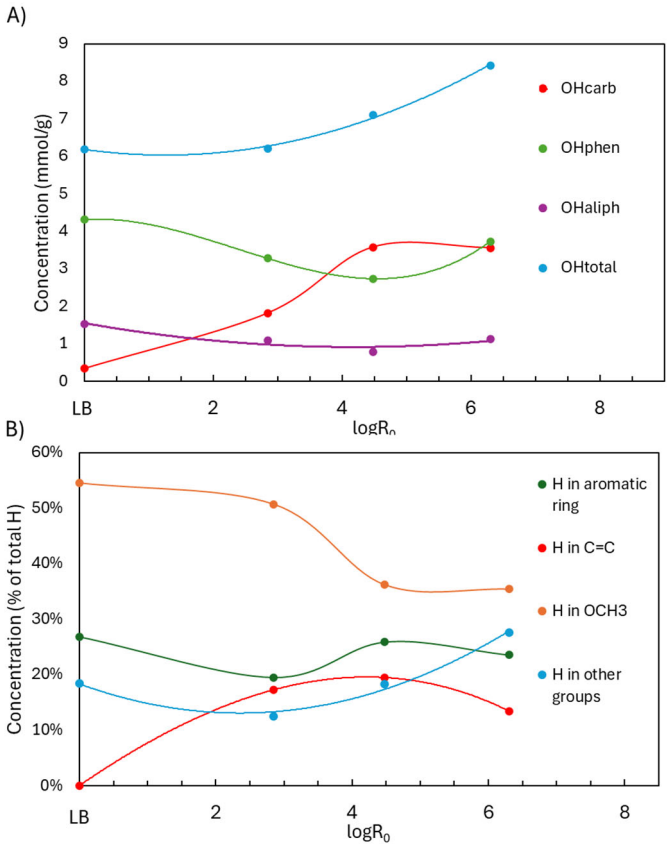


**Figure 4.** $^{1}H$ NMR and $^{31}P$ NMR analysis of functional groups in LB after acidic oxidative depolymerization under different severity factors.

$^{1}H$ NMR trends mirrored these changes (Figure 4.B). Below $logR_0 = 4.5$, $OCH_3$ protons declined due to demethoxylation, while C=C protons increased as side-chain and ring cleavages produced unsaturated compounds, including unsaturated esters and carboxylic/dicarboxylic acids. The mechanisms of demethylation and C=C formation are illustrated in Figure 3. Aromatic H content remained relatively stable, as the cleavage of rings was offset by the liberation of aromatic protons from broken side chains. Above $logR_0 = 4.5$, $OCH_3$ proton content stabilized, and both aromatic and C=C protons slightly decreased—likely due to saturation and transformation into aliphatic groups. At $logR_0 = 4.5$, H in $OCH_3$ dropped from 54.5% to 36.2%, H in C=C rose from 0.1% to 19.5%, and aromatic-H fell modestly from 26.9% to 25.9%. Thus, the aromaticity was preserved, $OCH_3$ groups decreased, and C=C groups were gained.

Elemental analysis (Table 1) further confirmed oxidative incorporation. C content declined steadily with severity, from 57.99% (LB) to 50.73%, 48.56%, and 46.48% at increasing temperatures. This was accompanied by a rise in O content from 32.86% to 43.46%, due to functionalization with OH, COOH, and C=O groups, as well as due to possible C reduction through gas-phase losses ($CO_2$, CO). H content showed minor variation. Based on this data and $OCH_3$ quantification, the empirical formula of the phenyl propane unit (PPU) for each depolymerized lignin was calculated. Despite demethoxylation reducing molar mass, the increase in oxygen content raised the PPU mass from 235.69 g/mol (LB) to 262.24, 255.60, and 271.28 g/mol for $logR_0$ values of 2.9, 4.5, and 6.3, respectively.

**Table 1.** Elemental analysis and empirical formula in LB after acidic oxidative depolymerization under different severity factors.

| Sample | $logR_0$ | C | H | O | S | N | PPU empirical formula | $Mw_{PPU}$ (g/mol) |
|---|---|---|---|---|---|---|---|---|
| LB | - | 57.9 ± 0.03 | 5.55 ± 0.02 | 32.86 ± 0.06 | 3.10 ± 0.24 | 0.52 ± 0.33 | $C_9H_{5.944}O_{2.461}S_{0.228}N_{0.087}(OCH_3)_{2.372}$ | 235.69 |

Preprints.org (www.preprints.org) | NOT PEER-REVIEWED | Posted: 31 March 2025 doi:10.20944/preprints202503.2415.v1



| | | | | | | | | |
|---|---|---|---|---|---|---|---|---|
| 50°C, 7 h | 2.85 | 50.73 ± 0.19 | 4.71 ± 0.02 | 39.41 ± 0.34 | 4.66 ± 0.28 | 0.51 ± 0.17 | $C_9H_{6.083}O_{4.373}S_{0.382}N_{0.095}(OCH_3)_{2.085}$ | 262.24 |
| 60°C, 3 h | 4.48 | 48.56 ± 0.16 | 4.36 ± 0.02 | 41.90 ± 0.26 | 4.57 ± 0.21 | 0.62 ± 0.11 | $C_9H_{7.102}O_{5.350}S_{0.365}N_{0.113}(OCH_3)_{1.343}$ | 255.60 |
| 70°C, 2 h | 6.30 | 46.48 ± 0.09 | 4.71 ± 0.20 | 43.46 ± 0.12 | 4.84 ± 0.25 | 0.52 ± 0.12 | $C_9H_{8.254}O_{5.860}S_{0.410}N_{0.101}(OCH_3)_{1.508}$ | 271.28 |

$logR_0$: severity factor; PPU: phenylpropane unit; $Mw_{PPU}$: molecular weight of the phenylpropane unit.

Thermal analysis (TGA and DTG) in Figure 5 revealed clear trends correlating with depolymerization degree. The 150–230 °C region, associated with volatile monomers, showed increasing degradation: 10.6%, 10.5%, and 12.9 wt.% at 50 °C, 60 °C, and 70 °C, respectively. These closely matched the GPC-estimated monomer yields of 12.4%, 9.8%, and 13.4%. The 230–310 °C region, likely involving oligomeric species and functional group breakdown, showed a smaller increase in degradation with temperature (13.3%, 13.3%, 14.7%). In the 310–400 °C region, linked to high-molecular-weight oligomers, degradation remained similar across samples (~15.2–15.8%), though DTG peaks flattened with increasing severity. The residual mass at 600 °C remained comparable to LB (36.1%), with minor variation across depolymerized samples (36.3–38.4%).

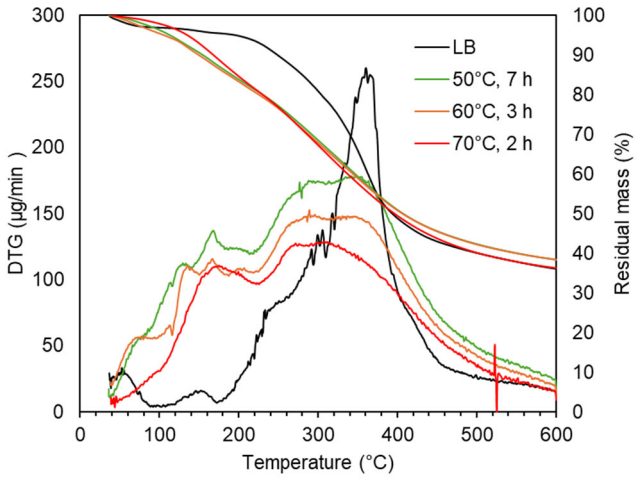


**Figure 5.** TG and DTG curves in LB after acidic oxidative depolymerization under different severity factors.

Some of the monomers formed during depolymerization at the three temperatures were identified by GC-FID/(TOF-MS) (Table 2). The results from $^{31}P$ NMR showed a clear prevalence of OHphen over OHaliph, which suggests a greater presence of aromatic rather than aliphatic compounds. However, the identification of monomers by GC-FID/(TOF-MS) showed a predominance of aliphatic compounds, which likely arise from the multiple transformations occurring, including the cleavage of side chains and the cleavage of aromatic rings (Figure 3). The absence of dimers and trimers in the GC-FID/(TOF-MS) analysis could be attributed to a lack of solubility and/or volatility even after derivatization.

**Table 2.** GC-FID/(TOF-MS) identification of monomers derived from acidic oxidative depolymerization in LB and KL.

| | **Formula** | **Mw (g/mol)** | **LB 50°C, 7 h logR0 2.85** | **LB 60°C, 3 h logR0 4.48** | **LB 70°C, 2 h logR0 6.30** | **KL 60°C, 3 h logR0 4.48** |
|---|---|---|---|---|---|---|
| **Alcohols** | - | - | 2.01% | 2.04% | 1.44% | 1.33% |
| Ethylene glycol | $C_2H_6O_2$ | 62.08 | 2.01% | 2.04% | 1.44% | 1.33% |

Preprints.org (www.preprints.org) | NOT PEER-REVIEWED | Posted: 31 March 2025 doi:10.20944/preprints202503.2415.v1



| | | | | | | |
|---|---|---|---|---|---|---|
| Hydroxycarboxylic acids | - | - | 14.73% | 14.73% | 16.93% | 19.21% |
| Lactic acid | $C_3H_6O_3$ | 90.09 | 0.72% | 0.74% | 0.53% | 4.24% |
| Glycolic acid | $C_2H_4O_3$ | 76.06 | 9.15% | 9.27% | 11.40% | 8.94% |
| 2-Hydroxybutyric acid | $C_4H_8O_3$ | 104.12 | 0.43% | 0.44% | 0.22% | 3.10% |
| Glyceric acid | $C_3H_6O_4$ | 106.09 | 3.03% | 3.07% | 3.15% | 1.95% |
| Malic acid | $C_4H_6O_5$ | 134.10 | 1.40% | 1.42% | 1.63% | 0.97% |
| **Dicarboxylic acids** | - | - | 50.28% | 53.40% | 56.21% | 29.36% |
| Oxalic acid | $C_2H_2O_4$ | 90.04 | 27.14% | 27.52% | 15.72% | 8.88% |
| Propanedioic acid | $C_3H_4O_4$ | 104.07 | 19.96% | 22.65% | 36.26% | 18.23% |
| Succinic acid | $C_4H_6O_4$ | 118.10 | 1.76% | 1.79% | 2.19% | 1.26% |
| Ethylmalonic acid | $C_5H_8O_4$ | 132.13 | 1.42% | 1.44% | 2.03% | 0.99% |
| **Esters** | - | - | 1.65% | 1.68% | 11.28% | 6.43% |
| Methyl 2-hydroxypropanoate | $C_4H_8O_3$ | 104.12 | 0.18% | 0.18% | 1.88% | 0.99% |
| Monomethyl succinate | $C_5H_8O_4$ | 132.13 | n.d. | n.d. | 3.35% | 1.28% |
| Methyl 2-hydroxyethyl malonate | $C_6H_{10}O_5$ | 162.16 | n.d. | n.d. | 4.88% | 2.71% |
| Butyl 6-methylheptanoate | $C_{12}H_{24}O_2$ | 200.36 | 1.47% | 1.49% | 1.17% | 1.45% |
| **Lactones** | - | - | 0.54% | 0.55% | 2.39% | 2.69% |
| 3-Hydroxy-3-hydroxymethyl-dihydro-2(3H)-furanone | $C_5H_8O_4$ | 132.13 | 0.39% | 0.40% | 2.08% | 0.55% |
| 2,3,4,5-Tetrahydroxypentanoic acid-1,4-lactone | $C_5H_8O_6$ | 164.11 | n.d. | n.d. | n.d. | 0.42% |
| Erythrono-1,4-lactone | $C_4H_6O_4$ | 118.10 | 0.15% | 0.15% | 0.31% | 1.32% |
| D-Erythro-Pentonic Acid, γ-Lactone | $C_5H_8O_5$ | 148.11 | n.d. | n.d. | n.d. | 0.41% |
| **Monosaccharides** | - | - | 12.16% | 10.87% | 2.10% | 29.91% |
| D-Arabinopyranose | $C_5H_{10}O_5$ | 150.15 | 0.78% | 0.79% | 0.00% | 1.40% |
| β-Arabinopyranose | $C_5H_{10}O_5$ | 150.15 | 0.00% | 0.00% | 0.72% | 1.58% |
| D-ribose | $C_5H_{10}O_5$ | 150.15 | 1.44% | 0.00% | 0.55% | 0.99% |
| D-xylose | $C_5H_{10}O_5$ | 150.15 | 4.76% | 4.83% | 0.42% | 11.95% |
| β-D(-)-Lyxopyranose | $C_5H_{10}O_5$ | 150.15 | 5.18% | 5.25% | 0.41% | 11.56% |
| Methyl xylopyranoside | $C_6H_{12}O_5$ | 164.18 | n.d. | n.d. | n.d. | 2.43% |
| **Aromatics** | - | - | 12.89% | 12.57% | 2.73% | 2.48% |
| 2,6-Dimethoxyhydroquinone | $C_6H_4(OH)(OCH_3)_2$ | 170.18 | 0.50% | n.d. | 0.19% | 0.34% |
| Vanillic acid | $C_6H_4(OH)(COOH)(OCH_3)$ | 168.16 | 1.91% | 1.93% | 0.74% | 0.89% |
| Benzoic acid, 4-hydroxy-3,5-dimethoxy- | $C_6H_4(OH)(COOH)(OCH_3)_2$ | 198.19 | 0.32% | 0.32% | n.d. | n.d. |
| Protocatechuic acid | $C_6H_4(OH)(COOH)(OCH_3)$ | 154.13 | 0.70% | 0.71% | 0.39% | n.d. |
| Syringic acid | $C_6H_4(OH)(COOH)(OCH_3)_2$ | 198.19 | 3.38% | 3.43% | 0.30% | n.d. |
| Acetyl syringic acid | $C_9H_{10}O_5$ | 240.23 | 1.16% | 1.17% | 0.40% | 1.26% |

Preprints.org (www.preprints.org) | NOT PEER-REVIEWED | Posted: 31 March 2025 doi:10.20944/preprints202503.2415.v1



| | | | | | | |
|---|---|---|---|---|---|---|
| Phthalic acid, di(2,3-dimethylphenyl) ester | $C_6H_4(CO_2R)_2(OCH_3)_2$ | 350.44 | 0.40% | 0.40% | 0.25% | n.d. |
| 4,4'-Methylenedi-2,6-xylenol | $C_{14}H_{14}O_2$ | 214.28 | 3.70% | 3.75% | 0.46% | n.d. |
| 3-Hydroxy-7,8,2',3'-tetramethoxyflavone | $C_{19}H_{18}O_7$ | 358.37 | 0.83% | 0.84% | n.d. | n.d. |
| **Other monomers** | - | - | 5.74% | 3.97% | 6.93% | 8.58% |

Among the monomers identified, there was a strong formation of low-molecular-weight dicarboxylic acids: 50.28, 53.40, and 55.21 wt.% for $logR_0$ values of 2.9, 4.5, and 6.3. Oxalic and propanoic acids, containing 2 and 3 C atoms, were most abundant, suggesting oxidative side-chain cleavage and possible ring cleavage followed by decarboxylation of the resulting muconic acids. Notably, no muconic acids (i.e., six-carbon dicarboxylic acids) were detected. Considering the estimated proportion of monomers from GPC analysis, the content of dicarboxylic acids in the solid depolymerized samples would be 6.23 wt.% (50°C, 7 h, $logR_0$ 2.9), 5.23 wt.% (60°C, 3 h, $logR_0$ 4.5), and 7.5 wt.% (70°C, 2 h, $logR_0$ 6.3).

Additionally, hydroxycarboxylic acids were abundant, likely originating from the breakdown of side chains attached to the aromatic rings [18]. Their presence was greater under more severe conditions, being 14.76, 14.93, and 16.93 wt.% for $logR_0$ values of 2.9, 4.5, and 6.3, respectively. The major hydroxycarboxylic acids identified were glycolic acid, glyceric acid, and malic acid. As shown by the ATR-FTIR spectra, under more severe conditions, the formation of esters via esterification between COOH and OH, catalyzed by the acidic conditions, was favored. The total content of esters increased from 1.64 wt.% ($logR_0$ 2.9) to 11.28 wt.% ($logR_0$ 6.3). The predominant esters were methyl 2-hydroxyethyl malonate and monomethyl succinate.

Regarding the total content of monomers identified, minor compounds included alcohols such as ethylene glycol (up to 2.05 wt.%) and lactones. Lactones are compounds formed by the cyclization of a COOH group with an OH group. Their presence increased as treatment severity increased, going from 0.54 wt.% ($logR_0$ 2.9) to 2.39 wt.% ($logR_0$ 6.3). Notably, the presence of monosaccharides was also observed, reaching 12.16 wt.% when the treatment conditions were milder ($logR_0$ 2.9) and decreasing to 2.10 wt.% under more severe conditions ($logR_0$ 6.3). This observation is unexpected, given that LB is of high purity and contains minimal carbohydrate content. One alternative hypothesis is that these sugar-like structures are formed via acidic hydrolysis and subsequent decarboxylation of lactones.

Finally, it is worth noting the content of aromatic compounds. The aromatics identified do not represent the entirety of those present but do provide an idea of which are the ones with lower molecular weight. The proportion of monomers identified as aromatics was 12.89, 12.57, and 2.73 wt.% for $logR_0$ values of 2.9, 4.5, and 6.3, respectively. The decrease in aromatic monomers under more severe conditions seems to indicate that these units undergo further transformations, ranging from ring cleavage to some degree of repolymerization. The most abundant aromatic monomers that could be identified, after 60C-3h, were 4,4'-methylenedi-2,6-xylenol (up to 3.75 wt.%), syringic acid (up to 3.43 wt.%), acetyl syringic acid (up to 1.17 wt.%) and vanillic acid (up to 1.93 wt.%). For instance, protocatechuic acid was also identified, which exhibits an interesting catechol functional group, with potential photoactivity and wide pharmacological activities.

### *2.2. Oxidative Depolymerization/Functionalization: Effect of Stirring and pH*

#### 2.2.1. Molecular Weight Distribution

To examine the influence of operational variables, depolymerization experiments were compared at 60°C for 3 h — selected as a reference condition due to the stabilization of functional group variations at this severity.

Preprints.org (www.preprints.org) | NOT PEER-REVIEWED | Posted: 31 March 2025 doi:10.20944/preprints202503.2415.v1



Lignin remains suspended, not dissolved, in acidic oxidative depolymerization. Given its high concentration (300 mg/mL), adequate stirring is essential for effective mass transfer and depolymerization. Without stirring, aggregates form, limiting contact between $H_2O_2$ and the solid. This was reflected in molecular weight distribution (Figure 6), where the unstirred reaction produced fewer dimers–trimers (20.5 vs. 25.8 wt.%) and more tetramers–decamers (68.6 vs. 62.2 wt.%), indicating lower depolymerization efficiency.

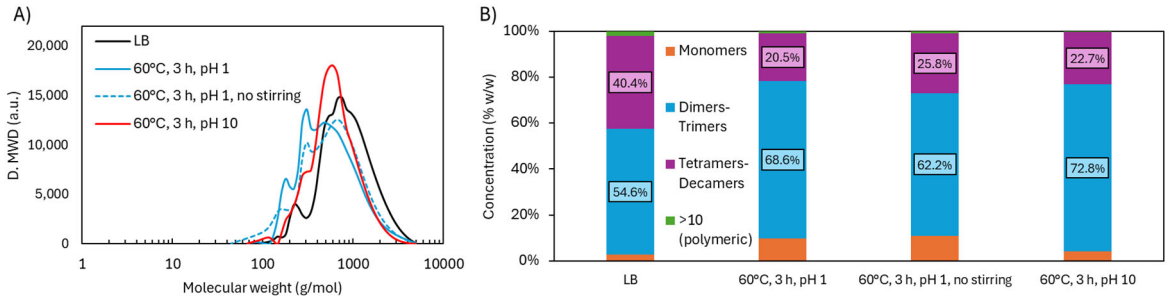


**Figure 6.** Molecular weight distribution in LB after oxidative depolymerization: effect of stirring and pH.

$H_2O_2$ is also active in alkaline media, particularly between pH 10–12.5 [11]. Here, pH 10 was used to balance oxidative power and minimize $H_2O_2$ decomposition. Under these conditions (60°C, 3 h), monomer content was much lower (4.1 wt.%) compared to acidic treatment (9.8 wt.%). Dimers–trimers and tetramers–decamers were slightly higher (72.8 and 22.7 wt.%, respectively), suggesting less fragmentation. This reduced monomer recovery can be attributed to: 1) repolymerization, promoted by lignin's solubility in alkaline media; 2) loss during precipitation, as monomers remained in solution upon pH adjustment to 2; and/or 3) incomplete depolymerization, due to greater structural stability under alkaline conditions. These phenomena—repolymerization, monomer loss during precipitation, and incomplete depolymerization—have been previously reported by other authors [13,14]. Monomer recovery from the liquid phase was considered, but high salt content (60 wt.%) in that fraction made it unviable. Molecular weight (Mw) and dispersity (Đ) values were 667 g/mol and 1.6 under acidic conditions, compared to 705.6 g/mol and 1.4 under alkaline conditions.

As a summary, efficient depolymerization under acidic conditions requires stirring to enhance contact; and alkaline depolymerization is less effective for monomer recovery unless a salt-free process is employed.

### 2.2.2. Structural Characterization (ATR-FTIR, 1H NMR, 31P NMR, EA, TGA)

This section compares the structural outcomes of oxidative depolymerization under acidic conditions without stirring and under alkaline conditions.

The ATR-FTIR spectra (Figure 7) of the non-stirred acidic experiment closely resemble those obtained with stirring, with only minor differences. A slightly lower intensity of the carbonyl (C=O) band at 1714 $cm^{-1}$ and a slightly higher intensity of the C–H in-plane aromatic signal at 1132 $cm^{-1}$ suggest lower formation of carboxylic acids and reduced demethoxylation.

Under alkaline conditions, the spectra resembled native LB, with minimal structural changes. The C=O oxidation peak appeared weakly, and no ester-related peak (1145 $cm^{-1}$) was detected, implying no esterification. Peaks for $OCH_3$-bound S units (1323 $cm^{-1}$) and C–H aromatic vibrations (1132 $cm^{-1}$) remained strong, indicating preserved aromatic substitution and minimal demethoxylation. The resulting lignin was structurally similar to the original LB, albeit with a slightly reduced Mw (708 vs. 979 g/mol).

Preprints.org (www.preprints.org) | NOT PEER-REVIEWED | Posted: 31 March 2025 doi:10.20944/preprints202503.2415.v1



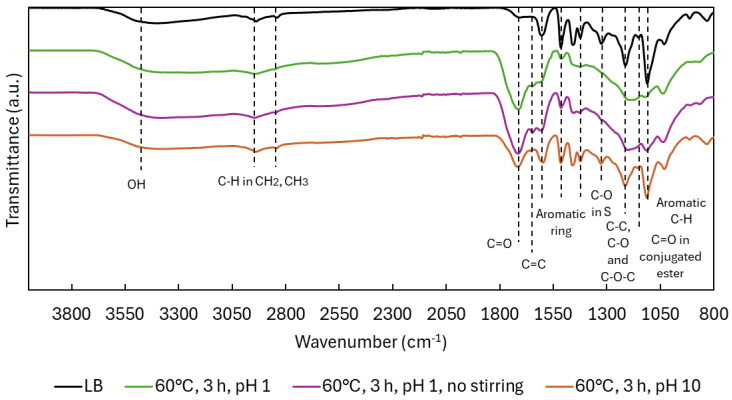


**Figure 7.** ATR-FTIR spectra in LB after oxidative depolymerization: effect of stirring and pH.

The $^{1}$H NMR analysis (Figure 8.A) reveals the distribution of protons across different functional groups. Under acidic conditions, demethoxylation occurred, reducing the $OCH_3$ group attached to the aromatic ring. This led to a slight increase in aromatic protons, compensating for the loss of aromatic H through other reactions, keeping its overall level fairly constant. The C=C group increased, likely due to the cleavage of aromatic rings and side chains. When no stirring was applied, the process efficiency decreased, resulting in less demethoxylation, a smaller increase in C=C, and a more pronounced decrease in aromatic H compared to stirred conditions.

Under alkaline conditions, the proportion of $OCH_3$ groups increased compared to acidic conditions. This could be due to the reduction of H from other groups, while $OCH_3$ remained intact, as observed in the ATR-FTIR spectra. Previous studies have shown that demethoxylation occurs under acidic conditions but not under alkaline conditions [17]. The C=C group appeared in smaller amounts, and aromatic H decreased. The formation of quinonic structures may explain the increase in C=C and the decrease in aromatic protons, while the $OCH_3$ groups remained intact. This process is promoted by the deprotonation of OHphen groups [11].

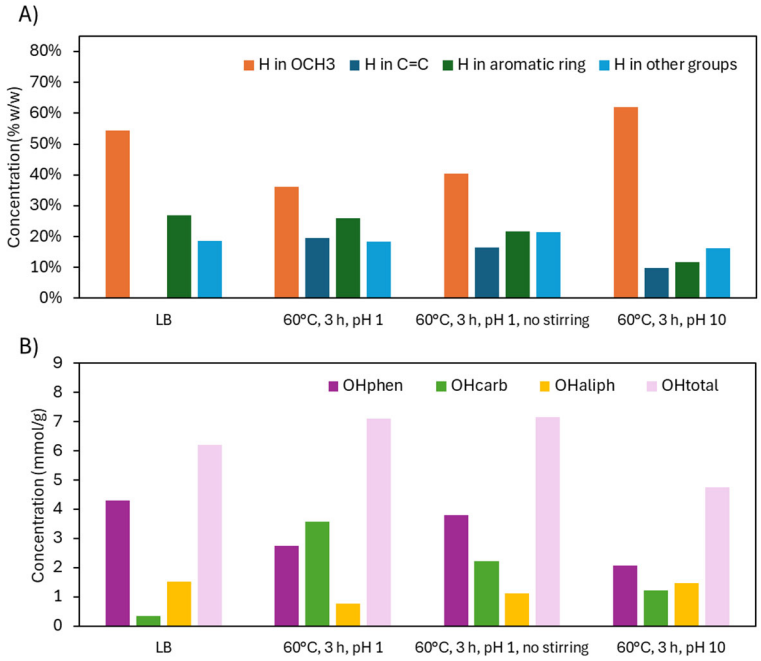


**Figure 8.** $^{1}$H NMR and $^{31}$P NMR analysis of functional groups in LB after acidic oxidative depolymerization: effect of stirring and pH.

Preprints.org (www.preprints.org) | NOT PEER-REVIEWED | Posted: 31 March 2025 doi:10.20944/preprints202503.2415.v1



The analysis of OH groups shows that the increase in OHcarb, indicating oxidation, was most pronounced under acidic conditions with stirring, followed by lower oxidation under conditions without stirring and even less under alkaline conditions. Despite less oxidation without stirring, depolymerization still occurred, decreasing the molecular weight of LB (from 979 to 730 g/mol) and increasing monomer-dimer-trimer proportion (from 57.4 to 73.1 wt.%), while maintaining a relatively high OHphen concentration (from 4.31 to 3.81 mmol/g).

In alkaline conditions, OHcarb increased slightly, likely due to phenolate ions being less prone to ring cleavage. However, alkaline conditions caused a significant decrease in OHphen (from 4.31 to 2.07 mmol/g), more so than in acidic conditions. This is likely due to the deprotonation of OHphen groups, increasing their reactivity and promoting the formation of quinonic structures. The marked reduction in OHphen resulted in a decrease in OHtotal (from 6.20 to 4.76 mmol/g), which was also reflected in the ATR-FTIR spectrum.

Elemental analysis (Table 3) shows that the non-stirred operation differs from the stirred one by a slightly lower increase in O content, resulting in less C loss and a smaller depletion of $OCH_3$ groups. In contrast, alkaline depolymerization exhibits minimal C loss and O gain, indicating lower depolymerization and functionalization, but confirming a slight increase in $OCH_3$ groups in the PPU. The molecular weight of PPU under acidic conditions was nearly identical with and without stirring (255.60 vs. 255.06 g/mol), despite differences in $OCH_3$ content. However, PPU obtained under alkaline conditions, with more $OCH_3$ groups but lower functionalization, had a lower molecular weight compared to the acidic depolymerization (246.26 vs. 255.60 g/mol).

**Table 3.** Elemental analysis and empirical formula of PPU in LB after acidic oxidative depolymerization: effect of stirring and pH.

| Sample | C | H | O | S | N | PPU empirical formula | $Mw_{PPU}$ (g/mol) |
|---|---|---|---|---|---|---|---|
| LB | 57.9 ± 0.03 | 5.55 ± 0.02 | 32.86 ± 0.06 | 3.10 ± 0.24 | 0.52 ± 0.33 | $C_9H_{5.944}O_{2.461}S_{0.228}N_{0.087}(OCH_3)_{2.372}$ | 235.69 |
| 60°C, 3 h, pH 1 | 48.56 ± 0.16 | 4.36 ± 0.02 | 41.90 ± 0.26 | 4.57 ± 0.21 | 0.62 ± 0.11 | $C_9H_{7.102}O_{5.350}S_{0.365}N_{0.113}(OCH_3)_{1.343}$ | 255.60 |
| 60°C, 3 h, pH 1, no stirring | 49.74 ± 0.08 | 4.58 ± 0.01 | 40.97 ± 0.14 | 4.23 ± 0.12 | 0.50 ± 0.06 | $C_9H_{6.956}O_{4.959}S_{0.337}N_{0.091}(OCH_3)_{1.571}$ | 255.06 |
| 60°C, 3 h, pH 10 | 56.71 ± 0.22 | 5.17 ± 0.08 | 34.89 ± 0.18 | 2.62 ± 0.15 | 0.61 ± 0.26 | $C_9H_{4.837}O_{2.732}S_{0.202}N_{0.107}(OCH_3)_{2.637}$ | 246.26 |

PPU: phenylpropane unit; $Mw_{PPU}$: molecular weight of the phenylpropane unit.

The TG and DTG curves (Figure 9) for acidic oxidative depolymerization show a high similarity between experiments with and without stirring, with only a slightly higher proportion of oligomeric material (310-400°C) in the non-stirred experiment.

Preprints.org (www.preprints.org) | NOT PEER-REVIEWED | Posted: 31 March 2025 doi:10.20944/preprints202503.2415.v1



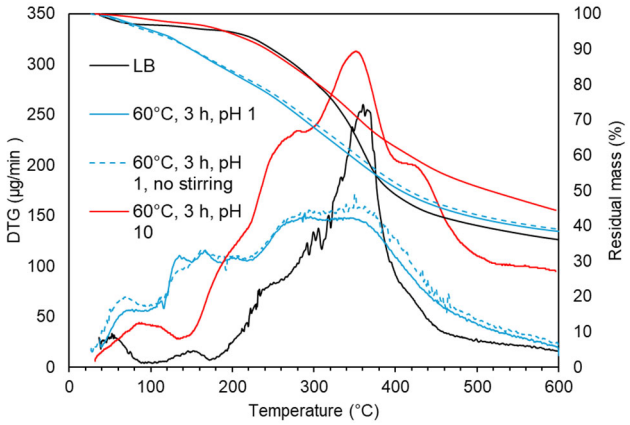


**Figure 9.** TG and DTG curves in LB after acidic oxidative depolymerization: effect of stirring and pH.

In contrast, under alkaline conditions the decomposition profile revealed distinct behaviors in different temperature regions. In the 150-230°C region, which is linked to the evaporation of volatile monomers, alkaline-treated lignin exhibited a lower weight loss (5.6 wt.%) compared to acidic conditions (10.5 wt.%), consistent with GPC monomer estimates of 4.1 wt.% and 9.8 wt.% for alkaline and acidic conditions, respectively. In the 230-310°C region, which involves decomposition of functional groups and low-molecular-weight species, alkaline-treated lignin showed a slightly lower weight loss (12.3 wt.%) compared to acidic conditions (13.3 wt.%). In the 310-400°C region, where maximum lignin degradation occurs (29.8 wt.% in LB), alkaline condition showed two degradation peaks: a major one at 360°C and another at 428°C. The second peak suggests the formation of thermally stable, crosslinked aromatic structures through repolymerization, consistent with previous studies [14]. This is supported by the higher degradation in the 400-600°C region for alkaline-treated lignin (17.9 wt.% vs. 12.4 wt.% under acidic conditions and 12.7 wt.% in LB), and a higher residual mass at 600°C (52 wt.% for alkaline-trated lignin compared to 38.4 wt.% under acidic conditions). These differences in thermal behavior arise from the distinct structural changes under acidic and alkaline conditions, with acidic depolymerization favoring side-chain cleavage and functional group introduction, and alkaline depolymerization retaining -$OCH_3$ groups and promoting thermal stability through repolymerization.

### *2.3. Oxidative Depolymerization/Functionalization of KL Versus LB*

#### 2.3.1. Evolution of the Molecular Weight Distribution

To evaluate the versatility of the oxidative depolymerization method, the same acidic protocol applied to LB was used on another lignin type, KL. Both lignins originated from *Eucalyptus globulus*, but differ in purity and protonation levels due to their extraction process.

In replicating the LB-pH1-60°C experiment with KL, the slurry pH reached 5 due to KL's lower protonation and higher salt content, which likely buffered the system. Although the medium was less acidic, the reaction was performed for comparison (KL-pH5-60°C, Table 1). As shown in Figure 10, no significant depolymerization occurred; the molecular weight distribution remained unchanged over time. This result aligns with the fact that $H_2O_2$ is largely inactive near neutral pH due to low radical generation.

Preprints.org (www.preprints.org) | NOT PEER-REVIEWED | Posted: 31 March 2025 doi:10.20944/preprints202503.2415.v1



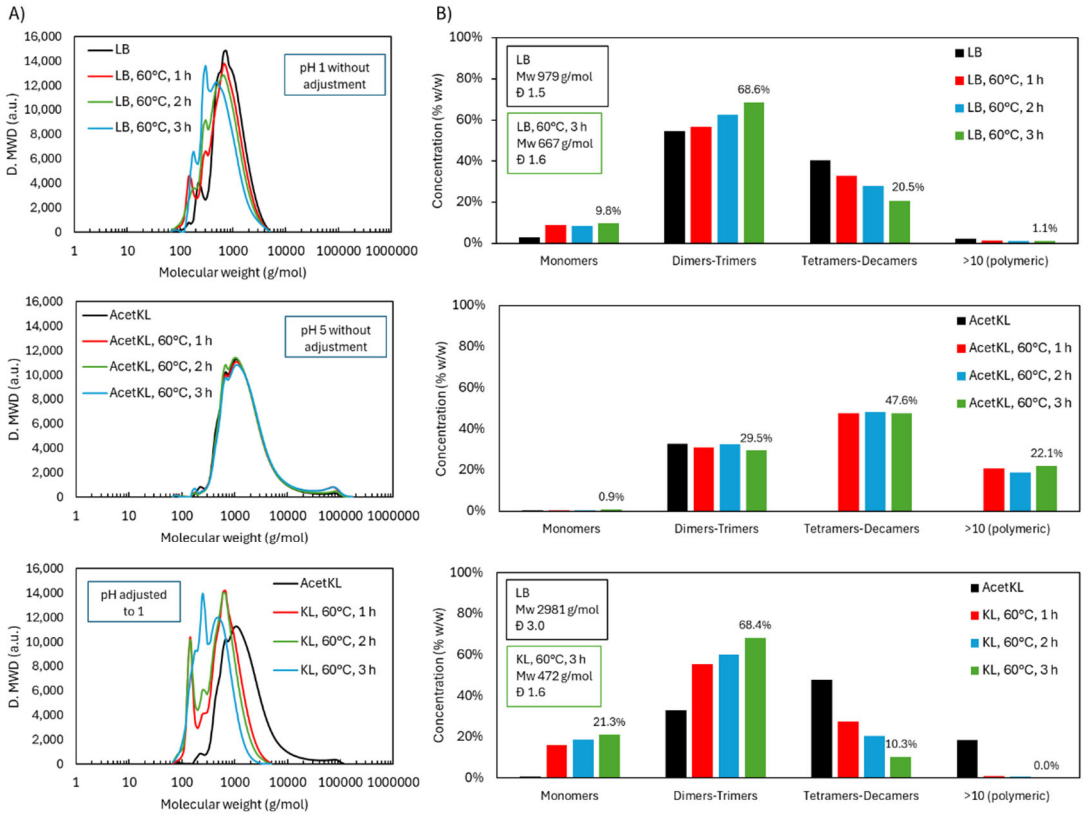


**Figure 10.** Molecular weight distribution during acidic oxidative depolymerization: LB *versus* KL.

KL's lower acidity posed a practical limitation, but using LB offers a key advantage: it introduces inherent acidity, avoiding external acid addition and minimizing salt content-beneficial for scalability and product purity. Due to solubility limitations, unmodified KL required acetylation for THF dissolution prior to GPC analysis.

To assess KL under acidic conditions, the pH was adjusted to 1 using 1 M $H_2SO_4$ (KL-pH1-60°C). Under these conditions, depolymerization proceeded effectively. Initially, monomers peaked, followed by rising dimer and trimer fractions. The final distribution was 21.3 wt.% monomers, 68.4 wt.% dimers-trimers, and 10.3 wt.% tetramers-decamers (treating KL), compared to 9.8 wt.% monomers, 68.6 wt.% dimers-trimers, and 20.5 wt.% tetramers-decamers (treating LB). KL showed a more pronounced reduction in tetramers-decamers and complete disappearance of the polymeric fraction, indicating higher depolymerization efficiency.

This enhanced efficiency in KL may be due to stable pH maintenance by strong acid ($H_2SO_4$), in contrast to LB's self-generated acidity, which may fluctuate during reaction. Additionally, catalytic impurities in KL may have promoted oxidative cleavage. Notably, depolymerized KL became THF-soluble without acetylation, suggesting altered solubility properties and reinforcing the structural transformation.

### 2.3.2. Structural Characterization (ATR-FTIR, $^{1}H$ NMR, $^{31}P$ NMR, TGA, and GC-FID/(TOF-MS))

The structural differences between the depolymerized LB and KL lignins were examined using multiple techniques.

ATR-FTIR spectra (Figure 11) showed similar patterns in both lignins post-depolymerization, with KL displaying a notably stronger C=O band at 1145 $cm^{-1}$ (conjugated esters). This suggests enhanced ester formation in KL, likely due to acid-catalyzed reactions facilitated by the stable pH maintained with $H_2SO_4$. These findings support the method's applicability to less pure lignins like KL, not just high purity LB.

Preprints.org (www.preprints.org) | NOT PEER-REVIEWED | Posted: 31 March 2025 doi:10.20944/preprints202503.2415.v1



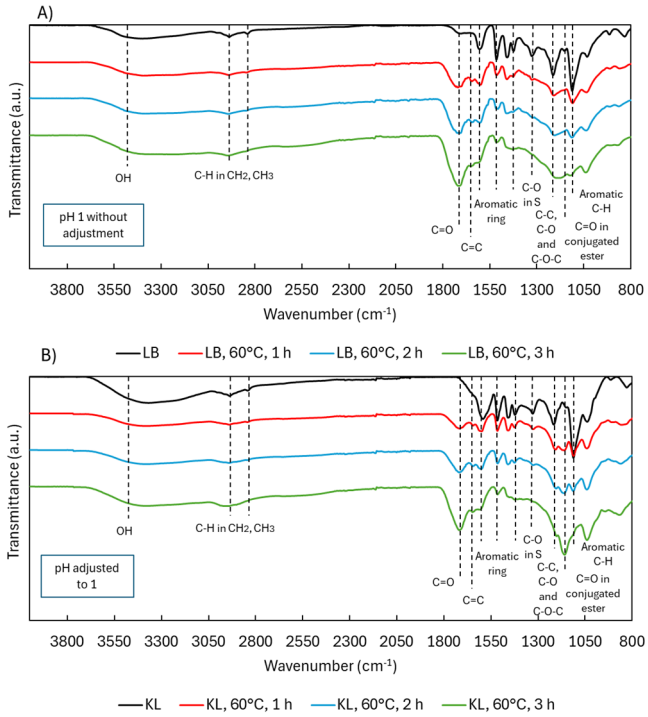


**Figure 11.** ATR-FTIR spectra during acidic oxidative depolymerization: LB *versus* KL.

$^{1}$H NMR analysis revealed that native KL contained more $OCH_3$ groups than LB, resulting in fewer aromatic protons due to increased substitution. After depolymerization, $OCH_3$ signals decreased—consistent with demethoxylation—while aromatic proton signals slightly increased in KL. C=C signals also increased but to a lesser extent than in LB, possibly because KL's OHphen groups were more stable under the stronger acid conditions, limiting quinone formation.

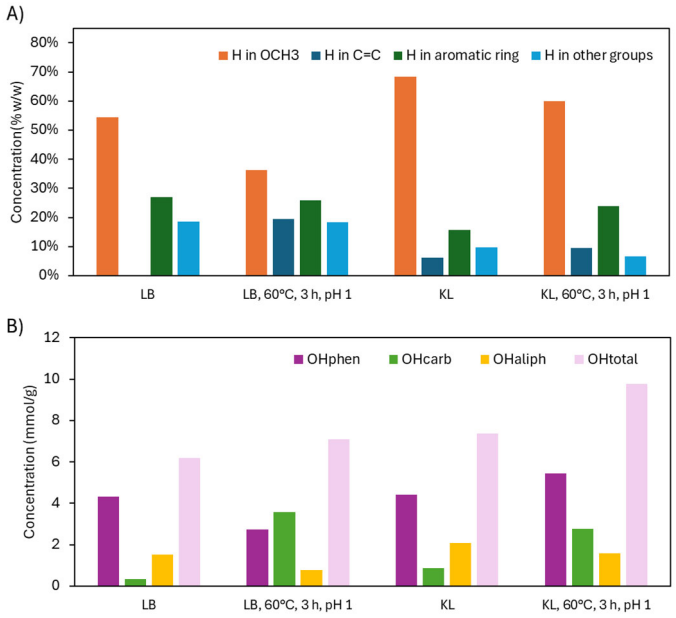


**Figure 12.** $^{1}$H NMR and $^{31}$P NMR analysis of functional groups after acidic oxidative depolymerization: LB *versus* KL.

$^{31}$P NMR (Figure 12.B) confirmed these trends. In KL, OHphen groups increased significantly (4.42 to 5.44 mmol/g), likely due to acid-stable conditions and potential aromatic hydroxylation. OHcarb groups also increased (0.86 to 2.76 mmol/g), while OHaliph groups decreased slightly (2.09

Preprints.org (www.preprints.org) | NOT PEER-REVIEWED | Posted: 31 March 2025 doi:10.20944/preprints202503.2415.v1



to 1.58 mmol/g), mirroring LB results. The OHtotal content rose from 7.37 to 9.78 mmol/g, indicating a more reactive and less sterically hindered lignin. This aligns with the sharp drop in molecular weight from 2981 to 472 g/mol.

TGA/DTG analysis (Figure 13) showed that LB degraded primarily at 310–400°C, while KL degraded at lower temperatures (230–310°C), likely due to its higher $OCH_3$ content, as demethoxylation typically occurs between 200–350°C. KL also had more residual mass at 600°C (52.3 wt.%) than LB (36.1 wt.%), likely reflecting higher impurity levels. After depolymerization, KL degraded at lower temperatures and had reduced residual mass (44.9 wt.%), consistent with lower molecular weight and possibly fewer impurities. In the 150–230°C range (monomer degradation), both lignins showed minor weight loss, but depolymerized LB lost 10.5 wt.% and KL 8.4 wt.%. Notably, no degradation peaks were observed between 400–600°C, suggesting no crosslinked aromatic structures formed under acidic conditions.

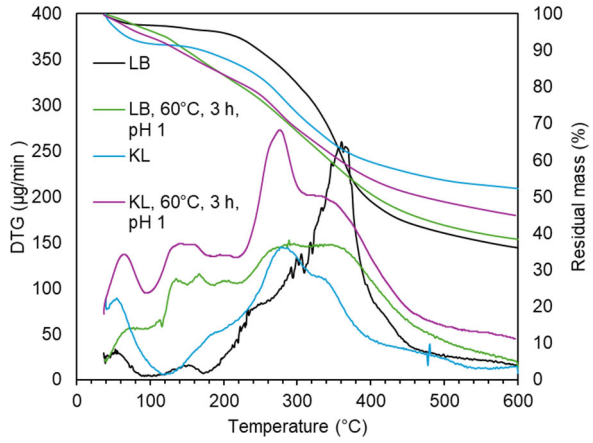


**Figure 13.** TG and DTG curves after acidic oxidative depolymerization: LB *versus* KL.

GC-FID/(TOF-MS) analysis (Table 4) confirmed differences in the monomeric product profiles. Depolymerized KL contained more hydroxycarboxylic acids than LB (19.21 vs. 14.73 wt.%), with glycolic acid being predominant in both. This may reflect more efficient side-chain cleavage under stable acidic conditions. Conversely, KL had far fewer dicarboxylic acids (29.36 vs. 53.40 wt.%), especially oxalic acid, possibly due to reduced aromatic ring cleavage or stronger acid conditions favoring ester formation. In the depolymerization of KL, the content of OHphen increased, suggesting hydroxylation and less aromatic ring cleavage compared to LB, possibly due to the higher molecular weight of KL (2981 vs. 979 g/mol).

Esterification under acidic conditions is supported by the higher ester content in KL (6.43 vs. 1.68 wt.%), with methyl 2-hydroxyethyl malonate as the main ester. KL also yielded more lactones (2.69 vs. 1.68 wt.%) and a notably higher monosaccharide content (29.9 vs. 10.87 wt.%), likely due to lignin–carbohydrate complexes co-precipitating during KL recovery from black liquor.

Aromatic monomers were present in low amounts in both cases, but even lower in KL (2.48 wt.%) than LB (12.57 wt.%). However, NMR and FTIR data suggest that aromaticity remains high in higher molecular weight fractions (dimers, trimers). In KL, the predominant aromatic monomers were acetyl syringyl (1.26 wt.%) and vanillic acid (0.89 wt.%), while LB showed higher levels of 4,4'-methylenedi-2,6-xylenol (3.75 wt.%), syringic acid (3.43 wt.%), and vanillic acid (1.93 wt.%).

### *2.4. Scale-Up of Acidic Oxidative Depolymerization of LB*

#### 2.4.1. Evolution of the Molecular Weight Distribution

To enable broader applications of depolymerized lignin, the acidic oxidative depolymerization of LB was scaled up under the same reference conditions: inherent acidity, 60 °C, and a 3 h reaction

Preprints.org (www.preprints.org) | NOT PEER-REVIEWED | Posted: 31 March 2025 doi:10.20944/preprints202503.2415.v1



time. The initial scale-up increased the reaction volume by a factor of 4, processing 12 g of LB in a reactor of the same type as the lab-scale setup, equipped with an oil bath and magnetic stirring. GPC results (Figure 14) confirmed that the molecular weight distribution remained virtually unchanged compared to the original scale. The product composition showed 8.8 wt.% monomers (vs. 9.8 wt.%), 71.9 wt.% dimers–trimers (vs. 68.6 wt.%), 18.7 wt.% tetramers–decamers (vs. 20.5 wt.%), and 0.6 wt.% polymeric fraction (vs. 1.1 wt.%). The Mw and Đ were also comparable: 667 g/mol and 1.6 at the smaller scale, versus 632 g/mol and 1.6 after the first scale-up.

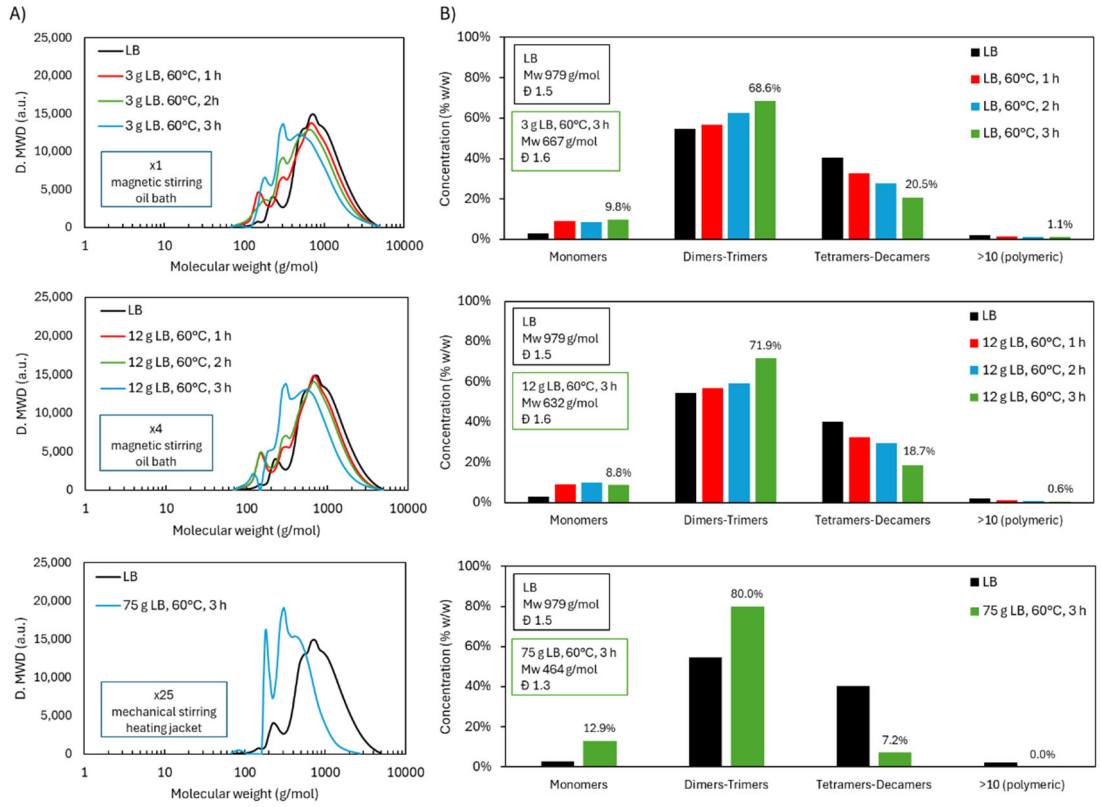


**Figure 14.** Molecular weight distribution of LB during acidic oxidative depolymerization under different scales (×1, ×4, ×25).

In the final stage, the process was scaled up 25-fold, treating 75 g of LB. This required a different reactor setup, using a water-jacketed vessel for temperature control and a motorized mechanical stirrer to ensure uniform mixing. These modifications resulted in markedly improved depolymerization efficiency. The GPC chromatogram revealed a substantial reduction in higher molecular weight fractions. The polymeric region was completely eliminated, and the tetramers–decamers fraction dropped to 7.2 wt.% (vs. 20.5 wt.%). Meanwhile, the dimers–trimers increased to 80.0 wt.% (vs. 68.6 wt.%) and the monomers to 12.9 wt.% (vs. 9.8 wt.%). This was reflected in a significantly lower Mw of 464 g/mol and a narrower dispersity (Đ = 1.3), compared to 667 g/mol and 1.6 at the original scale.

2.4.2. Structural Characterization (ATR-FTIR, $^{1}$H NMR, $^{31}$P NMR, and TGA)

Given the enhanced depolymerization observed at the ×25 scale, structural differences between scales were assessed. The ATR-FTIR spectra (Figure 15) were largely consistent between samples, though the scaled-up product showed a more intense band at 1145 cm$^{-1}$, associated with conjugated esters. This suggests an increase in esterification reactions, likely driven by a greater availability of COOH and OH groups under more homogeneous and efficiently stirred conditions. Improved mixing and temperature control likely played a key role in enhancing reaction uniformity and thus the extent of functionalization.

Preprints.org (www.preprints.org) | NOT PEER-REVIEWED | Posted: 31 March 2025 doi:10.20944/preprints202503.2415.v1



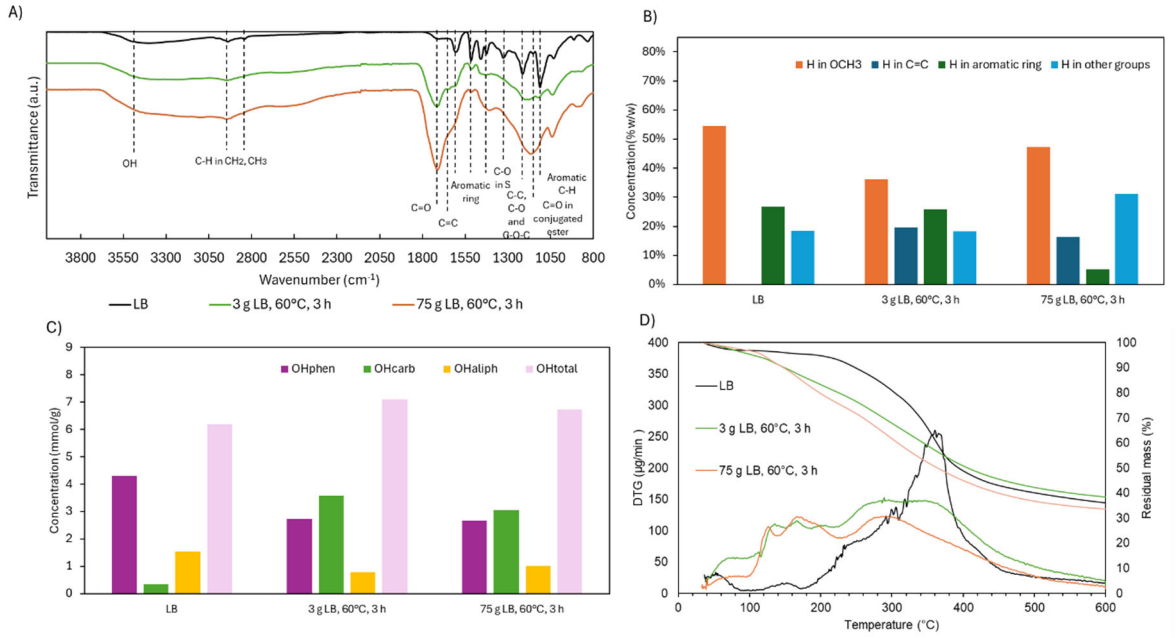


**Figure 15.** ATR-FTIR, $^{1}$H NMR, $^{31}$P NMR, and TGA results of LB after acidic oxidative depolymerization under different scales (×1, ×4, ×25).

$^{1}$H NMR analysis supported this interpretation. The scaled-up reaction showed a notable reduction in aromatic H content (5.2% vs. 25.9% at the smaller scale), likely due to increased ring cleavage. Simultaneously, H associated with aliphatic groups increased, indicating enhanced breakdown of side chains. Interestingly, $^{31}$P NMR revealed little difference in the distribution of OH groups between the two scales, including the phenolic fraction. This suggests that the drop in aromatic H content does not reflect a loss of aromatic structures per se, but rather a redistribution of H toward other functional groups, possibly with partial retention of $OCH_3$ groups.

TG and DTG curves further corroborated the observed structural changes. In the 150–230 °C range—associated with the evaporation or degradation of volatile monomers—the larger-scale sample showed slightly greater mass loss (14.8 wt.% vs. 10.5 wt.%), consistent with its higher monomer content. Between 230–310 °C, corresponding to degradation of $OCH_3$ and COOH groups and some dimers/trimers, mass loss was again marginally higher at scale (15.2 wt.% vs. 13.3 wt.%). In the primary degradation window of 310–400 °C, linked to aromatic breakdown, depolymerized samples showed a substantial reduction compared to native LB (29.8 wt.%). At the small and large scales, mass loss was 15.2 wt.% and 14.6 wt.%, respectively, suggesting comparable loss of aromaticity. Finally, in the 400–600 °C range, degradation remained relatively stable across all samples, decreasing slightly from 12.7 wt.% in native LB to 12.4 wt.% and 11.4 wt.% in the small- and large-scale products, respectively. Consistent with these thermal patterns and the increased degree of depolymerization, the residual mass at 600 °C was lower at the larger scale (33.6 wt.%) compared to the smaller-scale product (38.4 wt.%). This reduction reflects the formation of lower-molecular-weight, more oxidized, and thermally labile structures as the scale increases.

### *2.5. Reactivity of Depolymerized/Functionalized LB Through Radical Crosslinking*

Previous studies have demonstrated that OHphen groups in lignin can be activated via redox initiator systems such as $CaCl_2/H_2O_2$ under $O_2$-free conditions and moderate temperatures [26,27]. Given that depolymerized LB exhibits an enriched content of such functional groups, an activation test was carried out to assess their reactivity, specifically their capacity to form crosslinked structures.

As proof of concept, the product from the ×25 scale-up experiment (LB-pH1-60°C-×25, Table 4), hereafter referred to as DLB, was subjected to radical-induced crosslinking using this redox system. During activation, the OHphen—along with other reactive functionalities introduced during depolymerization, such as C=C and OHcarb—participated in the formation of a partially crosslinked

Preprints.org (www.preprints.org) | NOT PEER-REVIEWED | Posted: 31 March 2025 doi:10.20944/preprints202503.2415.v1



aromatic network. The resulting material, termed PolyActDLB, differs substantially from the original lignin and from DLB, as it represents a restructured and functionalized polymeric matrix.

Comprehensive characterization of PolyActDLB confirmed the occurrence of crosslinking. The molecular weight distribution (Figure 16.A) showed a pronounced increase, with Mw reaching 1375 g/mol, significantly higher than both DLB (464 g/mol) and the original LB prior to depolymerization (979 g/mol). The broadened dispersity (Đ = 3.43) further supports the formation of a highly branched polymer network, in contrast to the narrower distributions observed in LB and DLB (Đ = 1.33–1.54). Notably, PolyActDLB became insoluble in THF, unlike its precursors, necessitating a modified GPC protocol using DMF/LiCl as the solvent—additional evidence of successful crosslink formation and altered solubility behavior.

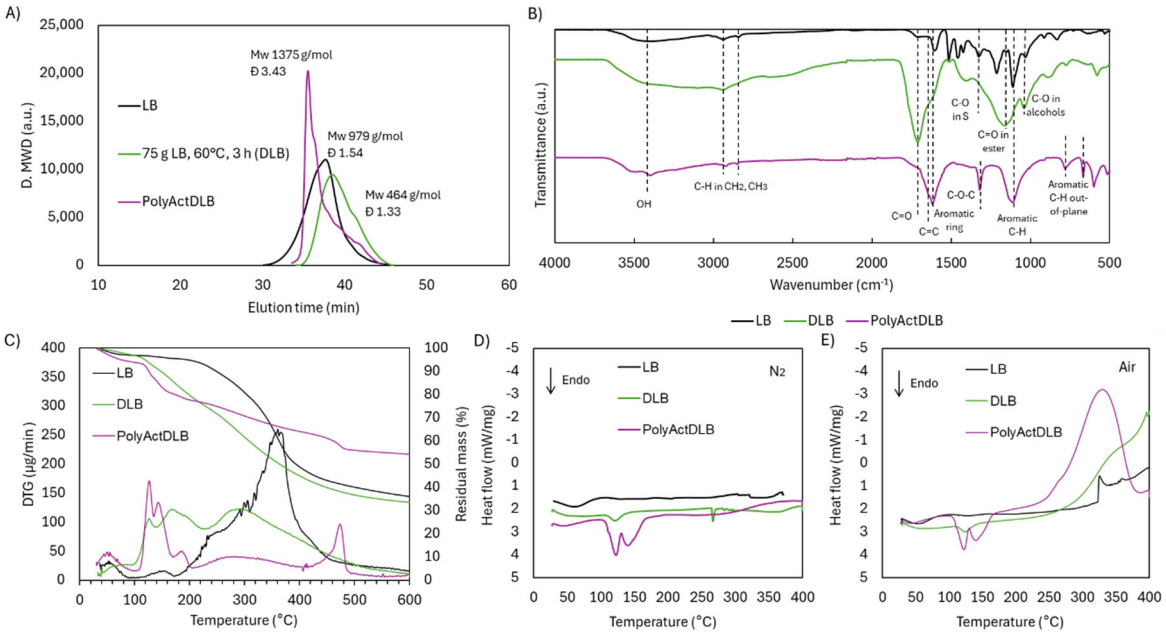


**Figure 16.** Molecular and structural characterization of lignin cross-linked matrix: A) molecular wight distribution, B) ATR-FTIR spectra, C) TG and DTG curves, D) DSC in $N_2$ atmosphere, and E) DSC in air atmosphere.

The ATR-FTIR spectra (Figure 16.B) revealed clear structural changes in PolyActDLB compared to both LB and DLB. The broad OH band between 3600–3000 $cm^{-1}$ was significantly reduced, likely due to the consumption of OH groups during the crosslinking reaction and the formation of new ether-type bonds. Interestingly, the prominent C=O peak at 1741 $cm^{-1}$, evident in DLB, was absent in PolyActDLB. This could indicate that carboxylic and dicarboxylic acid groups either participated in bond formation or were lost during aqueous-phase filtration, as these low-molecular-weight compounds are water-soluble.

Despite these transformations, the aromatic character of the lignin backbone was largely preserved. The band at 1604 $cm^{-1}$, associated with aromatic ring vibrations, remained prominent, as did the peak at 1132 $cm^{-1}$ corresponding to C–H in-plane deformation in aromatic systems. A notable change was the appearance of a peak at 1318 $cm^{-1}$, which is attributed to C–O–C stretching vibrations [28]. This peak may overlap with the signal typically assigned to the C–O bond in S units at 1323 $cm^{-1}$; however, C–O bond was present in the original LB and was almost completely reduced in DLB due to demethoxylation. Therefore, the 1318 $cm^{-1}$ peak could be primarily attributed to C–O–C linkages, likely formed during crosslinking via reactions between activated OHphen groups and other reactive moieties. Two new bands emerged at 782 and 664 $cm^{-1}$, assigned to C–H out-of-plane deformations in substituted aromatic rings [29]. These changes likely reflect alterations in ring substitution patterns or spatial orientation as a result of crosslinking.

Preprints.org (www.preprints.org) | NOT PEER-REVIEWED | Posted: 31 March 2025 doi:10.20944/preprints202503.2415.v1



Altogether, these spectroscopic features support the formation of a new bio-based aromatic polymer, of the polyether type. The proposed mechanism involves phenol activation followed by coupling, as illustrated below:

$$PPU–OH_{phen} \rightarrow PPU–O^* + H^+ \quad \text{(activation with } CaCl_2/H_2O_2\text{)}$$

$$PPU–O^* + PPU \rightarrow PPU–O–PPU^*$$

Thermal analysis by TGA and DTG (Figure 16.C) showed that PolyActDLB exhibits remarkable thermal stability. Only a small fraction of the material (6.9 wt.%) decomposed below 320 °C, likely corresponding to unreacted DLB monomers. Unlike LB and DLB, which undergo major decomposition in the 230–400 °C range, PolyActDLB showed minimal degradation in this region. Instead, its primary degradation peak appeared between 400–500 °C, and even then, mass loss was only 8.1 wt.%. The residual mass at 600 °C was significantly higher—54.2 wt.%, compared to 36.1 wt.% for LB and 33.6 wt.% for DLB—demonstrating the formation of a stable, crosslinked aromatic network, which could be attractive for high-temperature applications such as carbon fiber precursors or flame-retardant materials.

DSC analysis under a $N_2$ atmosphere (Figure 16.D) further highlighted the differences between PolyActDLB and its precursors. While LB and DLB lacked distinctive thermal transitions—typical of amorphous, heterogeneous materials—PolyActDLB displayed two endothermic events between 100–150 °C. These may correspond to the release of residual unreacted monomers, degradation of weak crosslinks, or evaporation of activation byproducts. These thermal events were also observed under air (Figure 16.E) and mirrored in the DTG curve.

Under oxidative conditions (Figure 16.E), thermal responses diverged significantly. LB exhibited a mild exothermic slope beginning around 300–350 °C, likely due to oxidation of labile functional groups. DLB showed a steeper exothermic slope beginning at a lower temperature (250–300 °C), consistent with its higher functionality and increased C=O and OH group content. In PolyActDLB, the exothermic event began earlier, between 200–250 °C, peaking in the 350–400 °C range. This suggests that the newly formed C–O linkages in the crosslinked matrix are more susceptible to oxidative cleavage, unlike the more resilient aromatic structures in LB and DLB.

The $^{1}H$ and $^{31}P$ NMR analyses showed interesting results (Supplementary Information file, Figure S10 and S20). On one hand, the proton distribution in the different functional groups of PolyActDLB revealed preservation of H in aromatic rings (5.0 vs. 5.2 wt.%, 6.00–9.00 ppm), indicating that the aromatic rings were largely retained. In contrast, the $OCH_3$ proton content decreased significantly (20.2 vs. 47.3 wt.%, 3.46–4.00 ppm). Since $OCH_3$ groups are generally stable to radical attack, this decrease could be due to demethoxylation under the acidic conditions used during crosslinking.

According to the proposed mechanism, the activated OHphen likely attack more reactive functional groups in lignin—those less stable than $OCH_3$—leading to the formation of new ether bonds. This may explain the increase in H content in ether-type environments (50.3 vs. 12.7 wt.%, 3.00–3.46 ppm). However, it is important to note that this region also overlaps with the residual water signal, so the actual value may be slightly overestimated.

Moreover, a marked decrease in H associated with alkene groups (C=C) was observed (0.8 vs. 16.3 wt.%, 4.00–5.80 ppm). This could be explained by the activation of vinyl groups in the presence of the radical initiator, leading to radical coupling and chain propagation as illustrated in the following mechanism:

$$PPU–CH_2\text{-}CH=CH_2 \rightarrow PPU–CH^*–CH=CH_2 \quad \text{(activation with } CaCl_2/H_2O_2\text{)}$$

$$PPU–CH^*–CH=CH_2 + PPU–CH_2–CH=CH_2 \rightarrow PPU–CH_2–CH=CH–CH_2–CH^*–CH_2–PPU$$

This reaction would explain both the decrease in alkene signals and the increase in $CH_2$-associated H (12.8 vs. 6.3 wt.%, 1.10–1.40 ppm). Other detected protons were attributed to $CH_3$ groups (4.6 wt.%, 0.8–1.0 ppm) and miscellaneous environments (5.3 wt.%).

The $^{31}P$ NMR results indicated that all the OHphen and OHaliph functional groups reacted during crosslinking, as their presence in PolyActDLB was below the detection limit. Only a small

Preprints.org (www.preprints.org) | NOT PEER-REVIEWED | Posted: 31 March 2025 doi:10.20944/preprints202503.2415.v1



amount of OHcarb (0.17 mmol/g) was detected, and this group is likely responsible for the low-intensity OH and C=O bands in the ATR-FTIR spectrum.

These results confirm the formation of a structurally distinct, thermally stable, and crosslinked aromatic material. The reactivity of depolymerized LB not only enhances functional group availability but also enables the design of lignin-based thermoset polymers with tailored properties.

## 3. Materials and Methods

### *3.1. Raw Material*

LB and black liquor, both from Kraft pulping of *Eucalyptus globulus* wood, were provided by RAIZ - Forest and Paper Research Institute (Portugal). Both materials were stored in a cool, dry, and dark place.

KL from black liquor was recovered applying precipitation and washing. For this, black liquor was maintained at 45°C for 1 h. Then, the pH was decreased down to 9.5 using a solution of $H_2SO_4$ and was stirred for 1 h so that lignin precipitation occurred. The precipitate was vacuum filtered and washed with acidic water at pH 3.0. The solid was dried under vacuum.

Non-stabilized hydrogen peroxide aqueous solution ($H_2O_2$, 30% w/v, Panreac) was used for the depolymerization experiments. Sodium hydroxide pellets (NaOH, Merck) and sulfuric acid 96% ($H_2SO_4$) were used to adjust pH. Pyridine (Merck) and acetic anhydride (analytical reagent grade, Fluka) were used for lignin acetylation. Hydrogen chloride (HCl, 1 M, Sigma–Aldrich) was used for precipitation of lignin solubilized at alkaline pH. Iron (II) sulfate heptahydrate ($FeSO_4 \cdot 7H_2O$, Panreac) was used as catalyst during radical crosslinking. Calcium chloride dihydrate ($CaCl_2 \cdot 2H_2O$, Sigma-Aldrich) and non-stabilized hydrogen peroxide aqueous solution ($H_2O_2$, 30% w/v, Panreac) were used for depolymerized lignin activation during crosslinking.

Tetrahydrofuran (THF, HPLC grade, Fisher chemical), dimethyl sulfoxide-d6 (DMSO-$d_6$, for NMR, Thermo scientific), chloroform-d (for NMR, Thermo scientific), cholesterol (Sigma-Aldrich), chromium(III) 2,4-pentanedionate (Cr(acac)3, Sigma-Aldrich), pyridine anhydrous (Sigma-Aldrich), 2-chloro-4,4,5,5-tetramethyl-1,3,2-dioxaphospholane (TMDP, Sigma-Aldrich), and N-Methyl-N-(trimethylsilyl)trifluoroacetamide (MSTFA, 97%, Thermo Scientific) were used as received for the characterization of lignin samples, depolymerized lignin, and the lignin-derived crosslinked matrix.

### *3.2. Oxidative Depolymerization of Lignin*

Depolymerization experiments were conducted to study the effect of (1) temperature, (2) stirring, (3) pH, and (4) type of lignin, followed by the scale-up of the best conditions. The experiments were carried out in 250 mL round-bottom glass reactor equipped with magnetic stirring, cooling condenser, and reagents inlet. The temperature was maintained via an oil bath controlled by a heating stirring plate with a Pt1000 sensor (LBX H20SQC, LBX instruments).

In the study of temperature and stirring, LB was suspended at a high concentration (300 mg/mL) in a 30% (w/v) $H_2O_2$ solution in water, therefore using a 1:1 (w/w) $H_2O_2$:lignin ratio. The reagents were mixed to a homogeneous slurry resulting in a pH close to 1 due to the acidic character of $H_2O_2$ and the protonated character of LB. The reactions were carried out at 50, 60, and 70°C, collecting periodic samples (Table 4). These samples, with a high concentration of solids, were dried at room temperature in petri dishes prior to characterization. In this way, all the depolymerization components, both water-soluble and non-water-soluble, were recovered. The operation at different temperatures and times is associated with a distinct severity factor, first mentioned by Overend and Chornet (1987) [30]. This term is commonly used to describe the combined effects of temperature and time on a given reaction, expressed by the following equation:

$$\log R_0 = \log[t\ (h) + (T\ (°C) - T_R) / 5], \quad (1)$$

Preprints.org (www.preprints.org) | NOT PEER-REVIEWED | Posted: 31 March 2025 doi:10.20944/preprints202503.2415.v1



Where $R_0$ is the severity factor, t is the reaction time (in hours), T is the temperature (°C), $T_R$ is the reference temperature (40°C), and 5 is a constant related to the activation energy of the specific process.

**Table 4.** Oxidative depolymerization operating conditions.

| Experiment | Type of lignin | Lignin (g) | 30% (w/v) $H_2O_2$ (mL) | Stirring | pH | T (°C) | Time (h) |
|---|---|---|---|---|---|---|---|
| LB-pH1-50°C | LB | 3 | 10 | Magnetic | 1 | 50 | 3, 5, 7 |
| LB-pH1-60°C | | | | | 1 | 60 | 1, 2, 3 |
| LB-pH1-70°C | | | | | 1 | 70 | 1, 2, 3 |
| LB-pH10-60°C | | | | | 10 | 60 | 1, 2, 3 |
| LB-pH1-0rpm-60°C | | | | No | 1 | 60 | 1, 2, 3 |
| KL-pH5-60°C | KL | 3 | 10 | Magnetic | 5 | 60 | 1, 2, 3 |
| KL-pH1-60°C | | | | | 1 | | |
| LB-pH1-60°C-×4 | LB | 12 | 40 | Magnetic | 1 | 60 | 1, 2, 3 |
| LB-pH1-60°C-×25 | | 75 | 250 | Mechanical | | | 3 |

LB: Lignoboost lignin, KL: Kraft lignin.

The influence of stirring was studied through its suppression in a depolymerization experiment at 60°C (LB-pH1-0rpm-60°C).

The effect of pH was studied by depolymerization under alkaline conditions because at neutral pH $H_2O_2$ loses its oxidizing character [11]. LB was first dissolved in NaOH solution with a NaOH:LB ratio 0.6:1 (w/w). After that, the corresponding volume of 30% w/v $H_2O_2$ was added dropwise to maintain a 1:1 (w/w) $H_2O_2$:LB ratio. The resulting pH was 10. Periodic samples were taken throughout the reaction. In this case, LB and the depolymerization products were soluble in the alkaline reaction medium. For the recovery of the samples, precipitation was carried out by decreasing the pH to 2 with a 0.1 M HCl. After precipitation, the samples were centrifuged, washed with distillated water, and dried under vacuum prior to characterization. The recovered solid was characterized, while the reaction products soluble in acidic water were mostly lost during centrifugation and washing, together with the salts formed as a result of the change in the pH for the precipitation process.

The effect of lignin type was studied by comparing the same acid depolymerization process applied to KL *versus* LB. For this purpose, KL was mixed with the corresponding volume of 30% (w/v) $H_2O_2$ so that the ratio $H_2O_2$:KL was 1. The result of the mixture was a homogeneous slurry whose pH was close to 5, proof of the higher alkaline character of KL versus LB. As a reference, depolymerization was carried out at these pH conditions, operating at 60°C and taking periodic samples (KL-pH5-60°C). To optimize the process and obtain a better comparison with LB, the process was repeated by adjusting pH to 1, the same as with LB, by adding 1M $H_2SO_4$ (KL-pH1-60°C). The reaction was carried out at 60°C and periodic samples were taken and, after drying at room temperature, were characterized.

Lastly, the acidic oxidative depolymerization process was scaled-up by selecting 60°C as the temperature. In a first test the reaction volume was increased by a factor of 4, using a round bottom glass reactor of the same type as in the previous experiments but with a 4 times larger volume (LB-pH1-60°C-×4). Magnetic stirring and an oil bath for heating were employed, as in the case of previous experiments (small quantities). Periodic samples were taken and dried at room temperature in larger petri dishes. Then, a scale-up was carried out by increasing the volume by a factor of 25 (LB-pH1-60°C-×25). This required the use of a 1 L glass reactor, coupled to a condenser, and with more precise temperature control thanks to a water jacket supplied by a thermal bath (Haake D1 L). Stirring efficiency was enhanced by coupling a motorized mechanical stirrer (DLH, VELP Scientifica). In this case, no periodical samples were taken, and all the final solid was collected and, as in the previous cases, dried on a glass plate at room temperature. The recovered solid, including water soluble and non-water soluble compounds, was characterized.

Preprints.org (www.preprints.org) | NOT PEER-REVIEWED | Posted: 31 March 2025 doi:10.20944/preprints202503.2415.v1



*3.3. Radical Crosslinking of the Depolymerized Lignin*

The product derived from the acidic oxidative depolymerization scale-up (LB-pH1-60°C-×25) was subjected to crosslinking using $CaCl_2/H_2O_2$ redox system as a radical initiator activating the OH groups of the sample. The reaction was carried out in a 250 mL three-neck Schlenk flask reactor equipped with magnetic stirring, cooling condenser, $N_2$ inlet, and reagents inlet. The temperature was maintained with an oil bath controlled by a heating-stirring plate with a Pt1000 sensor (LBX H20SQC, LBX instruments). The reaction took place at 55°C using water as the reaction medium. First, 1.362 g of $CaCl_2{\cdot}2H_2O$ (0.33:1 w/w $CaCl_2$:depolymerized lignin) was dissolved in 14 mL of distilled water. Then 3.0 g of depolymerized lignin (LB-pH1-60°C-×25) was added. The mixture was kept under magnetic stirring for 5 min under $N_2$ atmosphere. After that time, 0.566 mL of 30% (w/v) $H_2O_2$ (5.5:1 (w/v) depolymerized lignin:$H_2O_2$) was added. The mixture was kept under stirring and $N_2$ atmosphere for 2 h. After that time, the pH was adjusted to 3.0 with a NaOH solution and $FeSO_4$ (0.7 ppm of depolymerized lignin) previously dissolved in water was added. The reaction was maintained for 4 h under these conditions. The final mixture was vacuum-filtered and washed with distilled water. The washed solid was vacuum-dried overnight.

*3.4. Characterization of Lignoboost Lignin, Kraft Lignin, Depolymerized Lignin Samples, and Lignin-Derived Crosslinked Matrix*

The molecular weight distribution of LB, KL, and dried depolymerized lignin samples was determined by applying gel permeation chromatography (GPC) using a column (KF-803L; Shodex) protected by a pre-column (KF-G 4A; Shodex), maintained at 40°C. THF (HPLC grade) at a flow rate of 1 mL/min was used as mobile phase. The molecular weight distribution was determined using a UV detector (UV-4070, 280 nm) and the system was calibrated using eight polystyrene standards (62500 – 266 Da) from Agilent and one ethylbenzene standard (106 Da) from Ehrenstorfer. LB and depolymerized lignin samples were soluble in THF. On the contrary, KL and the samples derived from experiment KL-pH5-60°C required acetylation, performed according to the method described by Maitz et al. (2020) [31]. 0.5 g of each sample was dissolved in 3 mL of acetic anhydride and 3 mL of pyridine. The acetylation took place in an Anton Paar Monowave 50, at 150°C during 1 min. The product of the reaction was precipitated using 1 % (w/v) HCl, centrifuge, washed with distilled water to neutral pH, and dried under vacuum at 40°C. The acetylated dried solid, as well as the other lignin samples, were dissolved in THF for GPC analysis at a concentration of 1 mg/mL and were filtered before analysis (0.45 μm, PTFE).

The proportion of monomers in each sample was estimated following the method previously described by Ramos-Andrés et al. (2022) [32]. The detector intensity, assumed to be proportional to the analyte concentration, was used to integrate the chromatogram, and the area under the Mw distribution curve was divided into different molecular weight groups: monomers (<200 g/mol), dimers-trimers (201-873 g/mol), tetramers-decamers (874-2910 g/mol), and polymeric fraction (>2911 g/mol). The proportion of each group in the sample was calculated as the area in the corresponding region relative to the total area under the curve.

The lignin-derived crosslinked matrix was not soluble in THF. The GPC analysis was performed using two GPC columns in series (GRAM 1000 Å and 30 Å, PSS) protected by a pre-column (GRAM, PSS, 10 μm) and maintained at 70°C. A mobile phase of DMF/0.05 M LiCl was employed at a flow rate of 0.6 mL/min. UV detector was utilized to observe the molecular weight distribution, while RI detector was used to determine the weight-average molecular weight (Mw) and the polydispersity index (Đ). The system was calibrated using poly(methyl methacrylate) (PMMA) standards. LB and the product of the experiment LB-pH1-60°C-×25 were also analyzed by this method for comparison purposes. All the samples were dissolved in DMF/0.05 M LiCl at a concentration of 1 mg/mL and were filtered before analysis (0.45 μm, PTFE).

Thermogravimetric analysis (TGA) and derivative thermogravimetry (DTG) of LB, KL, depolymerized lignin samples, and lignin-derived crosslinked matrix were carried out using a

Preprints.org (www.preprints.org) | NOT PEER-REVIEWED | Posted: 31 March 2025 doi:10.20944/preprints202503.2415.v1



Hitachi STA7200 TGA/SDTA analyzer from Mettler Toledo. Approximately 5 mg of each sample were heated under a $N_2$ atmosphere (200 mL/min) at a rate of 10°C/min from 35 to 600°C.

The elemental analysis (EA) of LB and depolymerized samples from experiments LB-pH1-50, LB-pH1-60, LB-pH1-70, LB-pH1-0rpm-60, and LB-pH10-60 was performed with an EMA 502 elemental analyzer to assess the carbon, hydrogen, nitrogen and sulfur content. The oxygen content was estimated by subtracting the other percentages from 100%. The empirical formula of the phenyl propane (PPU) unit was determined from the results of EA and the content of methoxy groups determined using $^1$H NMR according to the method described by Sameni et al. (2016) [33].

The functional groups of LB, KL, dried depolymerized lignin samples, and lignin-derived crosslinked matrix were studied conducting attenuated total reflectance (ATR) – Fourier transform infrared spectroscopy (FTIR) on a Spectrum Two FT-IR spectrometer (PerkinElmer) equipped with a universal ATR (UATR) accessory. Approximately 5 mg of the solid sample was placed directly onto the diamond ATR crystal and pressed with a flat-tip anvil. Spectra were collected in the wavenumber range of 4000-400 $cm^{-1}$, with a resolution of 4 $cm^{-1}$ and 16 scans of data accumulation.

A Bruker Avance III 400 spectrometer (Karlsruhe, Germany) was used to conduct $^1$H NMR and $^{31}$P NMR analysis. For $^1$H NMR, 50 mg of dry samples were dissolved in 1 mL of DMSO-$d_6$ and sonicated for 60 min. $^1$H NMR was used to determine the content of aromatic hydrogen, methoxy groups ($OCH_3$) and hydrogen in alkene groups (C=C) in LB, KL, depolymerized lignin samples, and lignin-derived crosslinked matrix. $^{31}$P NMR was performed following the methodology described by Meng et al. (2019) [34], and it was used to determine the content of phenolic, aliphatic and carboxylic hydroxyl groups (OH) in LB, KL, and depolymerized lignin samples.

Before GC-FID/(TOF-MS) analysis, the solid samples of depolymerized lignin from experiments LB-pH1-50, LB-pH1-60, LB-pH1-70, KL-pH1-60°C were derivatized. To do this, 50 mg of the sample was dissolved in 1 ml of anhydrous pyridine under stirring, and then filtered (0.45 µM, PTFE) before being introduced into a GC vial. Next, 0.5 mL of the derivatizing agent, MSTFA, was added to the GC vial. The derivatization reaction was carried out at 80°C for 30 min. Afterward, 0.5 mL of anhydrous dichloromethane was added to the vial to dilute the sample. The monomers of the derivatized depolymerized lignin samples were identified using a two-column gas chromatography (GC) system. A volume of 1.0 µL of the sample was injected in split mode (1:10) into the GC×GC quadjet system (Leco), with the injector temperature set at 280°C. The carrier gas flow rate was 1.8 mL/min. The chromatographic system consisted of a primary column, Rxi-5ms (30 m length, 0.25 mm inner diameter, and 0.25 µm film thickness), connected to a secondary column, Rxi-17 Sil MS (1.6 m length, 0.25 mm inner diameter, and 0.25 µm film thickness). The primary oven temperature was initially set at 40°C for 3 min, followed by a heating ramp of 10°C/min to 300°C, where it remained for 11 min. The system was operated in a one-dimensional mode, with both Flame Ionization Detector (FID) and Time of Flight (TOF) Mass Spectrometry detectors used for identification. The FID detector temperature was set to 300°C, and the TOF transfer line temperature was set to 280°C, with an ionization energy of 70 eV.

## 4. Conclusions

Lignoboost lignin (LB) was successfully depolymerized and functionalized using oxidative depolymerization with $H_2O_2$ under inherently acidic conditions, without the use of organic solvents or catalysts. The effects of temperature, time, and stirring were studied. The LB was suspended at a high concentration (300 mg/mL) and its protonated character provided sufficient acidity for the depolymerization process. Conditions of 60°C and 3 h were enough to achieve good results, with a major fraction of aromatic dimers-trimers (68.6 wt.%) highly functionalized (2.75 mmol/g OHphen, 3.58 mmol/g OHcarb, 19.5 wt.% of H in -CH=CH-), as well as aliphatic dicarboxylic acids (53.4 wt.% of the monomers). The effect of pH was studied by comparing alkaline conditions (where LB is dissolved in the medium) to acidic conditions. Alkaline conditions partially oxidized LB but did not allow for adequate depolymerization or functionalization. The versatility of the process was demonstrated by applying the optimal acidic conditions to a less pure lignin, Kraft lignin (KL), which

Preprints.org (www.preprints.org) | NOT PEER-REVIEWED | Posted: 31 March 2025 doi:10.20944/preprints202503.2415.v1



required the addition of external acid but still yielded satisfactory results. The process was scaled up (×25) for LB, incorporating improvements in temperature control and mass transfer, resulting in a significant reduction in Mw and Đ from 979 g/mol and 1.5 to 464 g/mol and 1.3, respectively. The scaled-up solid product was subjected to radical crosslinking, leveraging the reactivity of OHphen and alkene groups, which can be activated to form a polyether-type crosslinked structure with high aromaticity and superior thermal stability compared to LB (54.2 wt.% *versus* 36.1 wt.% residual mass at 600°C).

**Author Contributions:** Conceptualization, M.C.L., T.N., A.C.M., and M.R.A.; methodology, M.C.L., T.N., A.C.M. and M.R.A.; validation, M.C.L. and M.R.A.; formal analysis, M.C.L., T.N., P.J.F.S. and M.R.A.; investigation, M.C.L., A.C.M. and M.R.A.; resources, P.J.F.S. and A.C.M.; data curation, M.C.L., T.L., P.J.F.S. and M.R.A.; writing—original draft preparation, M.C.L., T.L., P.J.F.S. and M.R.A.; writing—review and editing, M.C.L., A.C.M. and M.R.A.; visualization, M.C.L., T.L. and M.R.A.; supervision, A.C.M. and M.R.A.; project administration, A.C.M.; funding acquisition, A.C.M. All authors have read and agreed to the published version of the manuscript.

**Funding:** This research was funded by Fundação para a Ciência e a Tecnologia, project BioCFiber, [2022.08091.PTDC], https://doi.org/10.54499/2022.08091.PTDC. The authors thank Fundação para a Ciência e a Tecnologia for the PhD fellowship 2024.02028.BDANA (TN) and the support of CERENA, Strategic Project FCT-UIDB/04028/2025 and FCT-UIDP/04028/2025.

**Institutional Review Board Statement:** Not applicable.

**Informed Consent Statement:** Not applicable.
**Data Availability Statement:** Data will be made available on request.

**Acknowledgments:** The authors thank the company RAIZ - Forest and Paper Research Institute Lignoboost lignin and black liquor supply, Prof. Filipa Ribeiro and Cristian Castillo for making the GC-FID/(TOF-MS) analysis possible, Ivo Paulo for the elemental analysis, and Inês Faria for her contributions to the experimental work.

**Conflicts of Interest:** The authors declare no conflicts of interest.

## Abbreviations

The following abbreviations are used in this manuscript:

| | |
|---|---|
| LB | Lignoboost lignin |
| KL | Kraft lignin |
| DLB | Depolymerized Lignoboost lignin |
| PolyActDLB | Crosslinked polymer derived from DLB |
| PPU | Phenylpropane unit |
| Mw | Weight-average molecular weight |
| Đ | Dispersity index (Mw/Mn) |
| $\log R_0$ | Logarithmic severity factor |
| OHphen | Phenolic hydroxyl group |
| OHaliph | Aliphatic hydroxyl group |
| OHcarb | Carboxylic hydroxyl group |
| $OCH_3$ | Methoxy group |
| C=C / -CH=CH- | Aliphatic carbon-carbon double bond (alkene) |
| C=O | Carbonyl group (in ketones, acids, esters, etc.) |
| C-O-C | Ether linkage |
| THF | Tetrahydrofuran |
| DMSO-$d_6$ | Lignoboost lignin |
| MSTFA | N-Methyl-N-(trimethylsilyl)trifluoroacetamide (derivatizing agent) |

Preprints.org (www.preprints.org) | NOT PEER-REVIEWED | Posted: 31 March 2025 doi:10.20944/preprints202503.2415.v1



| | |
|---|---|
| TMDP | 2-Chloro-4,4,5,5-tetramethyl-1,3,2-dioxaphospholane (for $^{31}$P NMR) |
| $^{1}$H NMR | Proton nuclear magnetic resonance spectroscopy |
| $^{31}$P NMR | Phosphorus-31 nuclear magnetic resonance spectroscopy |
| ATR-FTIR | Attenuated total reflectance Fourier-transform infrared spectroscopy |
| GPC | Gel permeation chromatography |
| RI | Refractive index |
| UV | Ultraviolet |
| EA | Elemental Analysis |
| TGA/DTG | Thermogravimetric analysis/Derivative thermogravimetry |
| DSC | Differential scanning calorimetry |
| GC-FID/(TOF-MS) | Gas chromatography with flame ionization detector and time-of-flight mass spectrometry |

## References


1. Cao, Q.; Zhang, Y.; Chen, J.; Zhu, M.; Yang, C.; Guo, H.; Song, Y.; Li, Y.; Zhou, J. Electrospun Biomass Based Carbon Nanofibers as High-Performance Supercapacitors. *Ind. Crops Prod.* **2020**, *148*, 112181, doi:10.1016/j.indcrop.2020.112181.
2. Erfani Jazi, M.; Narayanan, G.; Aghabozorgi, F.; Farajidizaji, B.; Aghaei, A.; Kamyabi, M.A.; Navarathna, C.M.; Mlsna, T.E. Structure, Chemistry and Physicochemistry of Lignin for Material Functionalization. *SN Appl. Sci.* **2019**, *1*, 1–19, doi:10.1007/s42452-019-1126-8.
3. Andriani, F.; Lawoko, M. Oxidative Carboxylation of Lignin: Exploring Reactivity of Different Lignin Types. *Biomacromolecules* **2024**, *25*, 4246–4254, doi:10.1021/acs.biomac.4c00326.
4. More, A.; Elder, T.; Jiang, Z. Towards a New Understanding of the Retro-Aldol Reaction for Oxidative Conversion of Lignin to Aromatic Aldehydes and Acids. *Int. J. Biol. Macromol.* **2021**, *183*, 1505–1513, doi:10.1016/j.ijbiomac.2021.05.100.
5. Schorr, D.; Diouf, P.N.; Stevanovic, T. Evaluation of Industrial Lignins for Biocomposites Production. *Ind. Crops Prod.* **2014**, *52*, 65–73, doi:10.1016/j.indcrop.2013.10.014.
6. Hubbe, M.A.; Alén, R.; Paleologou, M.; Kannangara, M.; Kihlman, J. Lignin Recovery from Spent Alkaline Pulping Liquors Using Acidification, Membrane Separation, and Related Processing Steps: A Review. *BioResources* **2019**, *14*, 2300–2351, doi:10.15376/biores.14.1.hubbe.
7. Gärtner, A.; Gellerstedt, G.; Tamminen, T. Determination of Phenolic Hydroxyl Groups in Residual Lignin Using a Modified UV-Method Anna. *Nord. Pulp Pap. Res. J.* **1999**.
8. Zhang, Y.; Jiang, M.; Zhang, Y.; Cao, Q.; Wang, X.; Han, Y.; Sun, G.; Li, Y.; Zhou, J. Novel Lignin–Chitosan–PVA Composite Hydrogel for Wound Dressing. *Mater. Sci. Eng. C* **2019**, *104*, 110002, doi:10.1016/j.msec.2019.110002.
9. Qu, W.; Huang, Y.; Luo, Y.; Kalluru, S.; Cochran, E.; Forrester, M.; Bai, X. Controlled Radical Polymerization of Crude Lignin Bio-Oil Containing Multihydroxyl Molecules for Methacrylate Polymers and the Potential Applications. *ACS Sustain. Chem. Eng.* **2019**, *7*, 9050–9060, doi:10.1021/acssuschemeng.9b01597.
10. Rodrigues, A.E.; Vega-Aguilar, C.A.; Filomena Barreiro, M. Effect of Methoxy Substituents on Wet Peroxide Oxidation of Lignin and Lignin Model Compounds: Understanding the Pathway to C4 Dicarboxylic Acids. *Ind. Eng. Chem. Res.* **2021**, *60*, 3543–3553, doi:10.1021/acs.iecr.0c05085.
11. More, A.; Elder, T.; Jiang, Z. A Review of Lignin Hydrogen Peroxide Oxidation Chemistry with Emphasis on Aromatic Aldehydes and Acids. *Holzforschung* **2021**, *75*, 806–823, doi:10.1515/hf-2020-0165.
12. Ahmad, Z.; Dajani, W.W. Al; Paleologou, M.; Xu, C. Sustainable Process for the Depolymerization/Oxidation of Softwood and Hardwood Kraft Lignins Using Hydrogen Peroxide under Ambient Conditions. *Molecules* **2020**, *25*, doi:10.3390/molecules25102329.
13. Junghans, U.; Bernhardt, J.J.; Wollnik, R.; Triebert, D.; Unkelbach, G.; Pufky-Heinrich, D. Valorization of Lignin via Oxidative Depolymerization with Hydrogen Peroxide: Towards Carboxyl-Rich Oligomeric Lignin Fragments. *Molecules* **2020**, *25*, doi:10.3390/molecules25112717.

Preprints.org (www.preprints.org) | NOT PEER-REVIEWED | Posted: 31 March 2025 doi:10.20944/preprints202503.2415.v1




14. Ruwoldt, J.; Skunde, R.; Tanase-Opedal, M.; Syverud, K. Carboxylation of Lignin by Oxidation with Hydrogen Peroxide and Its Use as Emulsion Stabilizer. *Ind. Crops Prod.* **2025**, *223*, 120019, doi:10.1016/j.indcrop.2024.120019.
15. Kim, J.-C.; Choi, J.-H.; Kim, J.-H.; Cho, S.-M.; Park, S.-W.; Cho, Y.-M.; Park, S.-Y.; Kwak, H.W.; Choi, I.-G. Development of Lignin-Based Polycarboxylates as a Plasticizer for Cement Paste via Peracetic Acid Oxidation. *BioResources* **2020**, *15*, 8133–8145, doi:10.15376/BIORES.15.4.8133-8145.
16. Li, X.; Zhang, Y. Metal Catalyst-Free Oxidative C–C Bond Cleavage of a Lignin Model Compound by H2O2 in Formic Acid. *ChemSusChem* **2020**, *13*, 1740–1745, doi:10.1002/cssc.201903180.
17. Vega-Aguilar, C.A.; Barreiro, M.F.; Rodrigues, A.E. Lignin Conversion into C4 Dicarboxylic Acids by Catalytic Wet Peroxide Oxidation Using Titanium Silicalite-1. *Ind. Crops Prod.* **2021**, *173*, 114155, doi:10.1016/j.indcrop.2021.114155.
18. Sun, S.; Qiu, X.; Hao, S.; Ravichandran, S.; Song, J.; Zhang, W. Electrochemical Conversion of Lignin to Short-Chain Carboxylic Acids. *Green Chem.* **2023**, *25*, 3127–3136, doi:10.1039/d3gc00324h.
19. Bi, Z.; Li, Z.; Yan, L. Catalytic Oxidation of Lignin to Dicarboxylic Acid over the CuFeS2 Nanoparticle Catalyst. *Green Process. Synth.* **2018**, *7*, 306–315, doi:10.1515/gps-2017-0056.
20. Ding, R.; Wu, H.; Thunga, M.; Bowler, N.; Kessler, M.R. Processing and Characterization of Low-Cost Electrospun Carbon Fibers from Organosolv Lignin/Polyacrylonitrile Blends. *Carbon N. Y.* **2016**, *100*, 126–136, doi:10.1016/j.carbon.2015.12.078.
21. Mainka, H.; Täger, O.; Körner, E.; Hilfert, L.; Busse, S.; Edelmann, F.T.; Herrmann, A.S. Lignin - An Alternative Precursor for Sustainable and Cost-Effective Automotive Carbon Fiber. *J. Mater. Res. Technol.* **2015**, *4*, 283–296, doi:10.1016/j.jmrt.2015.03.004.
22. Ouyang, Q.; Cheng, L.; Wang, H.; Li, K. Mechanism and Kinetics of the Stabilization Reactions of Itaconic Acid-Modified Polyacrylonitrile. *Polym. Degrad. Stab.* **2008**, *93*, 1415–1421, doi:10.1016/j.polymdegradstab.2008.05.021.
23. Schorr, D.; Diouf, P.N.; Stevanovic, T. Evaluation of Industrial Lignins for Biocomposites Production. *Ind. Crops Prod.* **2014**, *52*, 65–73, doi:10.1016/j.indcrop.2013.10.014.
24. Gonçalves, S.; Martins, J.; Paiva, N.T.; Paiva, D.; Carvalho, L.H.; Magalhães, F.D. The Potential of Visible Spectroscopy as a Tool for the In-Line Monitoring of Lignin Methylolation. *Polymers (Basel).* **2023**, *15*, doi:10.3390/polym15010178.
25. Mainka, H.; Hilfert, L.; Busse, S.; Edelmann, F.; Haak, E.; Herrmann, A.S. Characterization of the Major Reactions during Conversion of Lignin to Carbon Fiber. *J. Mater. Res. Technol.* **2015**, *4*, 377–391, doi:10.1016/j.jmrt.2015.04.005.
26. Liu, X.; Xu, Y.; Yu, J.; Li, S.; Wang, J.; Wang, C.; Chu, F. Integration of Lignin and Acrylic Monomers towards Grafted Copolymers by Free Radical Polymerization. *Int. J. Biol. Macromol.* **2014**, *67*, 483–489, doi:10.1016/j.ijbiomac.2014.04.005.
27. Xu, X.; Xu, Y.; Deng, S.; Chen, X.; Essawy, H.; Lee, S.H.; Lum, W.C.; Zhou, X.; Zhang, J. Graft Copolymer of Tannin and Polyvinyl Alcohol with Acrylic Acid for the Preparation of Hydrophobic Biodegradable Film. *Prog. Org. Coatings* **2024**, *186*, 108090, doi:10.1016/j.porgcoat.2023.108090.
28. Falcão, L.; Araújo, M.E.M. Application of ATR-FTIR Spectroscopy to the Analysis of Tannins in Historic Leathers: The Case Study of the Upholstery from the 19th Century Portuguese Royal Train. *Vib. Spectrosc.* **2014**, *74*, 98–103, doi:10.1016/j.vibspec.2014.08.001.
29. Dutra, L.M.; Teles, P.H.V.; de Melo, N.F.; Nagata, N.; Almeida, J.R.G. da S. ATR-FTIR Spectroscopy Combined with Chemometric Tools for Rapid Distinction of Passiflora L. Species. *Rev. Bras. Plantas Med.* **2023**, *25*, 54–62.
30. Overend, R.P.; Chornet, E.; Gascoigne, J.A. Fractionation of Lignocellulosics by Steam-Aqueous Pretreatments. *Philos. Trans. R. Soc. London. Ser. A, Math. Phys. Sci.* **1987**, *321*, 523–536, doi:10.1098/rsta.1987.0029.
31. Maitz, S.; Schlemmer, W.; Hobisch, M.A.; Hobisch, J.; Kienberger, M. Preparation and Characterization of a Water-Soluble Kraft Lignin. *Adv. Sustain. Syst.* **2020**, *4*, doi:10.1002/adsu.202000052.

Preprints.org (www.preprints.org) | NOT PEER-REVIEWED | Posted: 31 March 2025 doi:10.20944/preprints202503.2415.v1



32. Ramos-Andrés, M.; Díaz-Cesteros, S.; Majithia, N.; García-Serna, J. Pilot-Scale Biorefinery for the Production of Purified Biopolymers Based on Hydrothermal Treatment in Flow-through Reactor Cycles. *Chem. Eng. J.* **2022**, *437*, doi:10.1016/j.cej.2022.135123.
33. Sameni, J.; Krigstin, S.; Sain, M. Characterization of Lignins Isolated from Industrial Residues and Their Beneficial Uses. *BioResources* **2016**, *11*, 8435–8456, doi:10.15376/biores.11.4.8435-8456.
34. Meng, X.; Crestini, C.; Ben, H.; Hao, N.; Pu, Y.; Ragauskas, A.J.; Argyropoulos, D.S. Determination of Hydroxyl Groups in Biorefinery Resources via Quantitative 31P NMR Spectroscopy. *Nat. Protoc.* **2019**, *14*, 2627–2647, doi:10.1038/s41596-019-0191-1.

**Disclaimer/Publisher's Note:** The statements, opinions and data contained in all publications are solely those of the individual author(s) and contributor(s) and not of MDPI and/or the editor(s). MDPI and/or the editor(s) disclaim responsibility for any injury to people or property resulting from any ideas, methods, instructions or products referred to in the content.